



HAL
open science

Adsorption behavior and mechanisms of the emerging antibiotic pollutant norfloxacin on eco-friendly and low-cost hydroxyapatite: Integrated experimental and response surface methodology optimized adsorption process

Sabrina Cheikh, Ali Imessaoudene, Jean-Claude Bollinger, Amar Manseri, Abdelkrim Bouzaza, Amina Hadadi, Nadia Hamri, Abdeltif Amrane, Lotfi Mouni

► To cite this version:

Sabrina Cheikh, Ali Imessaoudene, Jean-Claude Bollinger, Amar Manseri, Abdelkrim Bouzaza, et al.. Adsorption behavior and mechanisms of the emerging antibiotic pollutant norfloxacin on eco-friendly and low-cost hydroxyapatite: Integrated experimental and response surface methodology optimized adsorption process. *Journal of Molecular Liquids*, 2023, 392, pp.123424. 10.1016/j.molliq.2023.123424 . hal-04265209

HAL Id: hal-04265209

<https://hal.science/hal-04265209>

Submitted on 21 Dec 2023

HAL is a multi-disciplinary open access archive for the deposit and dissemination of scientific research documents, whether they are published or not. The documents may come from teaching and research institutions in France or abroad, or from public or private research centers.

L'archive ouverte pluridisciplinaire **HAL**, est destinée au dépôt et à la diffusion de documents scientifiques de niveau recherche, publiés ou non, émanant des établissements d'enseignement et de recherche français ou étrangers, des laboratoires publics ou privés.



Distributed under a Creative Commons Attribution - NonCommercial 4.0 International License

Adsorption behavior and mechanisms of the emerging antibiotic pollutant norfloxacin on eco-friendly and low-cost hydroxyapatite: Integrated experimental and response surface methodology optimized adsorption process

Sabrina CHEIKH^{a,b,*}, Ali IMESSAOUDENE^{a,b}, Jean-Claude BOLLINGER^c, Amar MANSERI^d, Abdelkrim BOUZAZA^e, Amina HADADI^a, Nadia HAMRI^{a,b}, Abdeltif AMRANE^f and Lotfi MOUNI^a

^a Laboratoire de Gestion et Valorisation des Ressources Naturelles et Assurance Qualité. Faculté SNVST, Université de Bouira, 10000 Bouira, Algeria

^b Département de Génie des Procédés, Faculté de Technologie, Université de Bejaïa, 06000 Bejaïa, Algeria

^c Laboratoire E2Lim (Eau Environnement Limoges), Université de Limoges, 123 Avenue Albert Thomas, 87060 Limoges, France

^d Centre de Recherche en Technologie des Semi-Conducteurs pour l'Energétique, 02 Bd Frantz Fanon, BP140, 7 Merveilles, Alger, Algérie

^e Laboratoire Sciences Chimiques de Rennes, Equipe Chimie et Ingénierie des Procédés, UMR 6226 CNRS, ENSCR, Avenue du Général Leclerc, 35700 Rennes, France

^f Université de Rennes, Ecole Nationale Supérieure de Chimie de Rennes, CNRS, ISCR - UMR 6226, F-35000 Rennes, France

*Corresponding author: E-mail address: sabrina.cheikh@univ-bejaia.dz (S. CHEIKH)

Phone: +213-674625274

Co-authors E-mail addresses

Ali IMESSAOUDENE : a.imessaoudene@univ-bouira.dz

Jean-Claude BOLLINGER : jean-claude.bollinger@unilim.fr

Amar MANSERI: amarmanseri@hotmail.com

Abdelkrim BOUZAZA: abdelkrim.bouzaza@enscr-rennes.fr

Amina HADADI: a.hadadi@univ-bouira.dz

Nadia HAMRI: n.hamri@univ-bouira.dz

Abdeltif AMRANE: abdeltif.amrane@univ-rennes1.fr

Lotfi MOUNI: l.mouni@univ-bouira.dz

Abstract

In this study, hydroxyapatite derived from bovine bone (nat-HAp) was used to remove norfloxacin antibiotic (NOR) from an aqueous solution. The nat-HAp properties were interpreted by analysis of the structure, specific surface area, functional groups, morphology, and composition. The pseudo-second-order kinetic and Langmuir isotherm suit the experimental data on NOR adsorption very well. Maximum absorption was shown to be 166.01 mg g⁻¹. Using a response surface methodology (RSM), the highest NOR elimination of 96.20 % was obtained under optimum conditions: NOR of 132.57 mg L⁻¹, pH of 7.88, nat-HAp dose of 0.99 g L⁻¹, and temperature of 25.06 °C. Thermodynamic studies demonstrated that the adsorption process was favorable, spontaneous, and exothermic. The value of standard enthalpy change (ΔH^0) shows that physisorption controlled the adsorption, and for this purpose, a viable mechanism for the adsorption of NOR onto nat-HAp was suggested. Based on the reusability experiment, the nat-HAp remained stable after four cycling runs. These results show that nat-HAp effectively absorbed NOR and might be a cost-effective alternative adsorbent to eliminate fluoroquinolone antibiotics during wastewater treatment.

Keywords: Adsorption; Norfloxacin; Natural hydroxyapatite; Optimization; response surface methodology; adsorption mechanism.

1. Introduction

The widespread usage of antibiotics has increased the presence of these substances in aquatic environments, which may negatively impact human and environmental health [1]. Antibiotics are often detected in surface water and wastewater [2]. Their toxicological effects on aquatic species and the resistance they can create in some bacterial strains, even at low doses, are becoming a growing concern [3]. Numerous antibiotics have properties of limited biodegradability and environmental persistence [4]; fluoroquinolone (FQ) antibiotics are an essential family of regularly used antibiotics. Norfloxacin (NOR, 1-ethyl-6-fluoro-1,4-dihydro-4-oxo-7-(1-piperazinyl)-3-carboxylic acid) is a fluoroquinolone antibiotic, broad-spectrum antibacterial compound with high antibacterial activity against both Gram-negative and Gram-positive bacteria through inhibition of DNA gyrase [5]. It is widely used in human and veterinary medicines [6]. However, norfloxacin had a slow rate of metabolism in both humans and animals, which led to the release of 40–90% of the drug's active metabolites into the environment via domestic sewage and farming wastewater [7]. In recent years, norfloxacin has been found in various aquatic environments, including drinking water [6–8]. As a broad-spectrum antibiotic, trace levels of norfloxacin in the environment may produce selection pressure on microbes, thereby increasing their antibiotic resistance [9,10], causing genotoxicity and teratogenesis, posing a threat to aquatic organisms and ecosystems [7,10], and finally posing a threat to public health. Considering the hazards of norfloxacin contamination in the aquatic environment, it was imperative to remove norfloxacin from the aquatic environment using a practical and efficient method.

Until now, various methods have been used to remove NOR from aqueous solution, such as adsorption [11], photocatalysis [12], Fenton oxidation [13], and electrochemical oxidation [14]. The most promising of these methods is adsorption owing to its environmental friendliness, low cost, simplicity, high efficiency, simple recovery, and reusability of the adsorbent [15,16]. Traditional adsorbents, such as biochar [17], activated carbon [18], alumina [19], zeolite [20], and others, are ineffective, have limited adsorption capabilities, and are challenging to renew for the removal of antibiotics [21]. Therefore, creating adsorbents with simple regeneration, high efficiency, and high adsorption capacity is crucial.

Hydroxyapatite [$\text{Ca}_{10}(\text{PO}_4)_6(\text{OH})_2$] is a widely used inorganic material in the fields of biology and medicine [22,23]. Due to its non-toxicity, bioactivity, biocompatibility, osteoconductivity, and non-immunogenic and non-inflammatory properties, it is the most promising biomaterial [24]. Due to its particular structure bestowing ionic exchange characteristics, low solubility in water, high stability in reducing and oxidizing conditions, and adsorption affinity towards several contaminants [25], it has been discovered to be an efficient adsorbent for environmental processes. This biomaterial has been used to remove potentially hazardous metal ions and chemical molecules from water [25,26]. It has been widely applied in chromatography to separate and purify nucleic acids and proteins [27]. Hydroxyapatite as a medication carrier has been the topic of extensive research [28].

Traditionally, one variable is changed simultaneously during experimental optimization while the others remain unchanged. Due to the large number of required trials, it is also difficult to conduct tests using every possible combination of study variables. By maximizing all influencing parameters collectively using a statistical experimental design, such as RSM [29], these limitations of a conventional technique can be overcome. RSM is a combination of statistical and mathematical approaches for constructing models, organizing experimentation, evaluating the impacts of variables, and determining the optimal conditions for factors to predict desired responses [30]. When developing an adsorption process, employing statistical experimental design techniques can lead to a reduction in process variability, an increase in product yields, a more precise confirmation of the output response to target requirements, as well as a reduction in both the amount of time required for development and the total cost of the project. Multiple researchers have described using RSM to optimize batch adsorption techniques [30,31]. Box-Behnken design (BBD) is RSM's most prevalent and efficient design. BBD has several benefits over the Doehlert and Central Composite designs, including the need for fewer experimental points and greater efficiency [32].

Therefore, the present study demonstrates that hydroxyapatite derived from bovine bone (nat-HAp) can effectively remove the antibiotic norfloxacin. The specific objectives of our investigation were as follows: (i) to prepare the low-cost hydroxyapatite material by pyrolysis (calcination) technique and to study its characteristics using X-ray diffraction (XRD), Nitrogen-Brunauer Emmett–Teller surface area analysis (N_2 -BET), Fourier transform infrared spectroscopy (FTIR), and field emission scanning electron microscopy coupled with energy dispersive spectroscopy (FESEM/EDX); (ii) to examine the applicability of different isotherm models (such as Langmuir, Freundlich, and Temkin) in order to determine the best-fit isotherm equation; (iii) To determine the utility of various kinetic models (such as pseudo-first-order and pseudo-second-order models); (iv) to study the feasibility of nat-HAp as an adsorbent for NOR antibiotic and optimize the adsorption using a Box–Behnken design-based (BBD) response surface methodology (RSM) with the Design Expert software (DES, Version 12, Stat-Ease, USA) under four independent variables including initial concentration, pH, adsorbent dosage, and temperature; (v) to discuss the mechanism through which NOR adsorbs to nat-HAp; (vi)

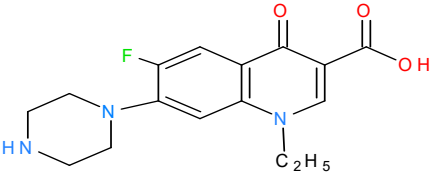
to study the thermodynamic properties (such as free Gibbs energy, enthalpy, and entropy); and (vii) to study the reusability of the nat-HAp.

2. Materials and methods

2.1. Materials

NOR was purchased from Sigma-Aldrich (Chem. Co., USA). The structure and relevant physicochemical properties of Norfloxacin are shown in Table 1. pH was adjusted using 0.1 mol L⁻¹ NaOH and 0.1 mol L⁻¹ HCl. All solutions were prepared using ultrapure water (Adrona, Millipore Milli-Q UV Plus, R = 18.25 MΩm).

Table 1. Norfloxacin properties

Molecular formula	C ₁₆ H ₁₈ FN ₃ O ₃
CAS number	70458-96-7
Purity	≥ 98% (TLC)
Molecular weight	319.33 g mol ⁻¹
pK_a	pK _{a1} = 6.22 ^(a) pK _{a2} = 8.51 ^(a)
Chemical structure	

(a) Cited by Hongsawat et al [33]

2.2. Preparation of adsorbent nat-HAp

The nat-HAp was prepared as reported in [34]. The fresh cortical bone of mature bovine (2-4 years old) was collected from the local slaughterhouse of Bouira (Algeria) and kept at - 20 °C. The bones were cleansed with water, and the soft portions of the bones were manually separated from the dense portions with a stiletto. The bones were then reduced to little bits using a cutter. Bones were cooked in water for two to three hours to facilitate the extraction of bone marrow and tendons [35–37]. To denature the protein, the bone fragments were dried in an oven at 80 °C for 72 hours [38]. The as-received dry bone samples were annealed in an electric furnace (Nabertherm GmbH Lilienthal, Germany) at 800 °C with a heating rate of 5 °C min⁻¹ and a

holding period of 3 hours [34,36]. Using a crusher, the bone fragments were subsequently crushed into small particles. The bone fragments were submitted to a ball milling procedure until the powder was fine enough. Sieving resulted in the production of bone powder. This study employed a powdered bone sample with a particle size of 100 μm .

2.3. Characterization of nat-HAp

The nat-HAp was characterized using different analytical techniques. The nat-HAp X-ray diffraction patterns (XRD) were produced and recorded on a D8 Advance Bruker X-ray Diffractometer (Germany) employing $\text{Cu K}\alpha$ radiation at an angle of 2θ ranging from 4° to 53° . With the aid of the JCPDS data, the phases were determined. The surface area of nat-HAp was measured using the N_2 -BET (Nitrogen-Brunauer Emmett–Teller) adsorption–desorption isotherms at 77K with an instrument from Micromeritics ASAP 2010 instrument corporation. Fourier transform infrared (FTIR) spectra were recorded on a Perkin Elmer FT-IR-300 spectrometer (Japan) using the KBr pellet method in the $400\text{--}4000\text{ cm}^{-1}$ spectral range. The morphology and composition of nat-HAp before and after norfloxacin adsorption were obtained by a field emission scanning electron microscope (FESEM: JSM- 6710FPlus, JEOL, Tokyo, Japan) equipped with an energy dispersive X-ray spectroscopy (EDX) system along with a brand Bruker X Flash® 6 | 10 Silicon Drift Detector (SDD). The pH of zero-point charge (pH_{ZPC}) was obtained using a method described elsewhere [34]. NOR antibiotic removal absorbance was measured at $\lambda_{\text{max}} = 275\text{ nm}$ using a double-beam UV–vis spectrophotometer (Agilent Technologies Cary 60 UV–vis).

2.4. NOR solution preparation

Fluoroquinolones, particularly NOR, can be difficult to dissolve in ultra-pure water, which might take several hours. In this study, the time necessary to prepare a solution was drastically reduced by using ultrasound-assisted technology [39]. NOR stock and working solutions were prepared and stored in a refrigerator in the dark. The stock solution was diluted to produce working solutions with concentrations between 5 and 200 mg L^{-1} .

2.5. Adsorption experiments

For adsorption experiments, 0.1g of nat-HAp was mixed with 100 mL of Norfloxacin (100 mg L^{-1}) solution at room temperature. We used 0.1 M HCl or 0.1 M NaOH to adjust the pH of the working solution to the desired value. The mixture was agitated at 200 rpm for 180 minutes at a predetermined contact time defined by kinetic research. Before and after adsorption, the concentration of NOR in the supernatant solution was measured using a UV/vis spectrophotometer at $\lambda_{\text{max}} = 275\text{ nm}$. All experiments were run in triplicate under the same conditions and the average values were presented. The maximum difference between the three values was less than 3% of the mean.

The adsorption capacity q_t (mg g^{-1}) and the removal efficiency (%) of NOR by nat-HAp were calculated at any time (t) by the following equations:

$$q_t = \left(\frac{C_0 - C_t}{m} \right) \times V \quad (1)$$

$$Y(\text{removal efficiency, \%}) = \left(\frac{C_0 - C_t}{C_0} \right) \times 100 \quad (2)$$

C_0 and C_t (mg L^{-1}) are the NOR concentrations at time zero and t , respectively. V (L) represents the volume of the solution, whereas m (g) represents the quantity of nat-HAp adsorbent employed.

2.6. Experimental design and optimization

In this research, the effects of operating conditions were optimized using BBD with three levels and four factors in RSM.

The input factor ranges are initial concentration (A: 100-180 mg L^{-1}), initial pH (B: 6-10), adsorbent dose (C: 0.5-1 g L^{-1}), and temperature (D: 25-55°C). These ranges were determined utilizing the results of preliminary studies. The experimental range and levels for the BBD model are shown in Table 2.

Table 2. Range and levels for the BBD model

Variables	Notation	Range and levels		
		Low level	Center level	High level
The initial concentration of NOR (mg L^{-1})	A	100	140	180
Initial pH of the solution	B	6	8	10
Adsorbent dose (g L^{-1})	C	0.50	0.75	1.00
Temperature ($^{\circ}\text{C}$)	D	25	40	55

The adsorption efficiency was determined by evaluating the affinity of nat-HAp for NOR. The experiment was designed by Design-expert 8.0.6.1 (Stat-Ease, 2012) (trial version) statistical software. Using a second-order polynomial model, all possible interactions between selected Box–Behnken model variables have been exposed:

$$Y = \beta_0 + \sum_{i=1}^n \beta_i X_i + \sum_{i=1}^n \beta_{ii} X_i^2 + \sum_{i=1}^{n-1} \sum_{j=i+1}^n \beta_{ij} X_i X_j + \varepsilon \quad (3)$$

where Y is the assumed response or output (Removal efficiency of NOR onto nat-HAp), n is the number of studied factors, i and j are the index numbers for pattern, β_i , β_{ii} , and β_{ij} the interaction coefficients of linear, quadratic, and second-order terms, respectively, and X_i , X_j are the values of the independent variables, and ε is the residual error. The R^2 value indicated the accuracy of the polynomial model's fit. The model Probability value (p -value) and Fisher

variation ratio (*F*-value) are the most important indications of the model's adequacy and significance [40].

2.7. Desirability function

A desirability function is only a mathematical approach for determining the optimal input parameter values and output response utilizing the optimal input parameter levels. The desirability function was created by Harrington [41] and then updated by Derringer and Suich [42]. The objectives included maximization, minimization, a target, a range, none (for responses only), and a precise value (factors only). Each included parameter must have a minimum and maximum level defined. Each objective can be allocated a weight to modify the form of its desirability function. The objectives are included in a global desirability function [43].

The desirability procedure consists of two steps: (a) determining the values of the independent variables and (b) optimizing the overall desirability of controllable factors [44]. The desirability function converts the response (y_n) into a 0 to 1 variable desirability function (d_i). The desirability 1 corresponds to the maximum (Max), while the desirability 0 corresponds to undesirable conditions or the minimum (Min).

Derringer and Suich [42] formulated the equation, which can be expressed as:

$$d_i = \left(\frac{Y - A}{B - A} \right)^{w_i}, A \leq Y \leq B \quad (4)$$

$$d_i = 1, \quad Y > B$$

$$d_i = 0, \quad Y < A$$

A and *B* in equation (4) represent the response's minimum and maximum obtained values, whereas w_i represents the weight. Calculating the geometric mean of the transformations of every individual desirability point yields the global desirability function, *D*.

$$D = [d_1^{v_1} \times d_2^{v_2} \times \dots \times d_n^{v_n}]^{1/n}, 0 \leq v_i \leq 1 \quad (i = 1, 2, \dots, n), \sum_{i=1}^n v_i = 1 \quad (5)$$

Where d_i represents the desirability of the response y_i ($i=1, 2, 3, \dots, n$) and v_i indicates the importance of responses.

2.8. Desorption studies

Desorption is the process of a substance leaving through a surface. This present study assessed the adsorbent's regeneration capability and reusability. Recycling an adsorbent is the most critical feature of a cost-effective method. To do this, antibiotic-adsorbed nat-HAp is produced by adsorbing 200 mg L⁻¹ antibiotic solution onto 1 g L⁻¹ nat-HAp at 25°C. After equilibration, antibiotic content in the filtrate was determined. Then, the adsorbent was added to 10 mL of purified water with varying pH (3, 5.5, 8.5, and 12). After shaking the solutions for approximately 60 min, the percentage of antibiotic desorbed into the solution was determined, and the desorption ratio was calculated using the following equation:

$$\text{Desorption (\%)} = (C_{des}/C_{ads}) \times 100 \quad (6)$$

Where C_{des} and C_{ads} are the antibiotic's desorbed and adsorbed concentrations (mg L^{-1}), respectively. The regenerated adsorbent was then thoroughly rinsed with ultrapure water until a pH neutralization was obtained. To prepare the regenerated material for usage in the next cycle of adsorption studies, it was heated at $60\text{ }^{\circ}\text{C}$ overnight and suspended in NOR solution at the same initial concentrations (200 mg L^{-1}). The adsorption–desorption cycle was repeated up to four times.

3. Results and discussion

3.1. Characterization of the adsorbent material

The XRD pattern of natural hydroxyapatite before norfloxacin adsorption was presented in Fig.1a. The components of the crystalline phase were identified using standard JCPDS cards accessible through the system software. The peaks at $2\Theta = 25.9^{\circ}$, 29.01° , 31.72° , 32.20° , 33° , 34.15° , 39.82° , 46.87° and 49.51° confirm the phase and purity of derived nat-HAp crystals.

The textural properties of the nat-HAp material were assessed using N_2 adsorption–desorption isotherms at $T=77\text{K}$. As depicted in Fig.1b, the nat-HAp material shows a type IV isotherm with an H_3 hysteresis loop according to the IUPAC classification [45], characteristic of mesoporous material [46–48]. The nat-HAp has a surface area of $8.5\text{ m}^2\text{ g}^{-1}$ and a pore volume of $16\text{ mm}^3\text{ g}^{-1}$; These results confirm earlier findings published by Piccirillo et al. [49] and Karoui et al. [50]. Both types of research demonstrated that biomass materials possess low surface values. Moreover, the pore size average of nat-HAp was 7.7 nm ($2\text{ nm} < \text{pore size} < 50\text{ nm}$), indicating the presence of mesopores [51,52].

FTIR spectra of free nat-HAp, free Norfloxacin, and loaded nat-HAp were utilized to elucidate the sorption mechanisms in greater detail (Fig. 2 a-c).

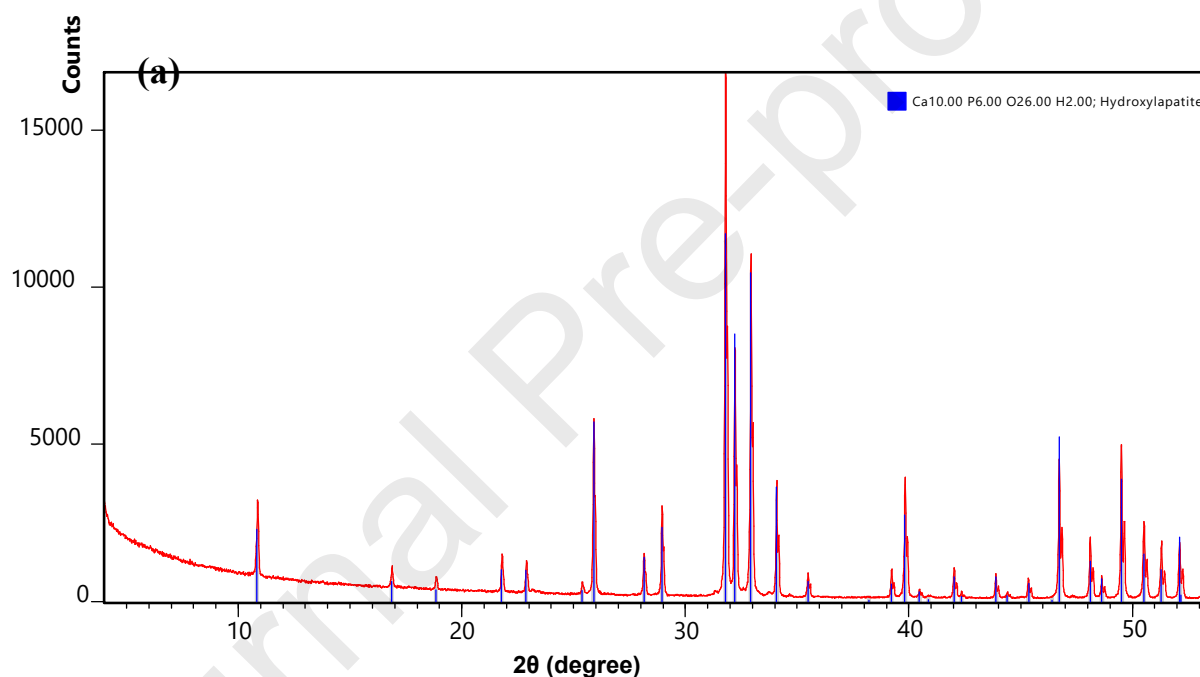
The spectrum of nat-HAp (Fig. 2a) was clearly defined, with peaks at 3572 and 635 cm^{-1} corresponding to the stretching vibrations of OH^- . Peaks at 1090 and 962 cm^{-1} are due to the stretching vibration of phosphate, and those observed at 605 , 570 , and 475 cm^{-1} are characteristic of the bending vibration of phosphate. The prominent peak at 1419 cm^{-1} results from water adsorption. In FTIR spectra, the low-intensity peak of carbonate groups is found at 1482 cm^{-1} due to the asymmetric stretching of the CO_3^{2-} group. These bands in the spectra correspond to the bands in the nat-HAp absorption spectrum and are in excellent correlation with nat-HAp data reported in the literature [34,53].

The spectrum of NOR (Fig. 2b) displayed the peaks at 1610 and 1575 cm^{-1} corresponding to the stretching vibration of the carboxylic and ketone groups of NOR [15,54]. The C–F stretching peak was detected at 1030 cm^{-1} , and two more peaks observed at 813 cm^{-1} and 1265 cm^{-1} were identified to the meta distribution of the aromatic protons and the C–O stretching vibration of carboxylic acid, respectively [55].

To gain insight into the interactions that happened during the sorption process, the FTIR spectrum of NOR-loaded nat-HAp was analyzed. The OH peaks corresponding to nat-HAp are absent in the spectra of nat-HAp following NOR adsorption (Fig. 2c), clearly apparent in the nat-HAp spectrum, as shown in Fig. 2a. The interaction between the COOH in the NOR molecule and the OH groups in the nat-HAp structure may be responsible for the observation of an elongated signal at 3500 cm^{-1} .

In addition, indications for the CH_2 and $=\text{CH}$ (stretching and bending vibrations, respectively) of the antibiotic about $3500\text{--}2500\text{ cm}^{-1}$ in Fig. 2c confirmed the presence of Norfloxacin on the natural hydroxyapatite structure [55]. The peaks ascribed to $\text{C}=\text{O}$ and COOH in the norfloxacin spectrum at 1575 and 1610 cm^{-1} , respectively (Fig. 2b), are also present in the nat-HAp -NOR spectrum, but they are combined with the water-assigned peak in the nat-HAp spectrum (Fig. 2a). New peaks at 1345 cm^{-1} and 1089 cm^{-1} are attributable to the protonated amino group in the piperazine moiety and C-F stretching, respectively. In addition, the C-H bending peaks for aromatic out-of-plane deformation showed at wave numbers 818 , 786 , and 749 cm^{-1} [56].

In contrast, additional vibrations corresponding to nat-HAp moieties remain in the spectrum (Fig. 2a) but with broad signals indicating the presence of the antibiotic. As mentioned above, all results demonstrate the effective NOR adsorption onto the nat-HAp adsorbent.



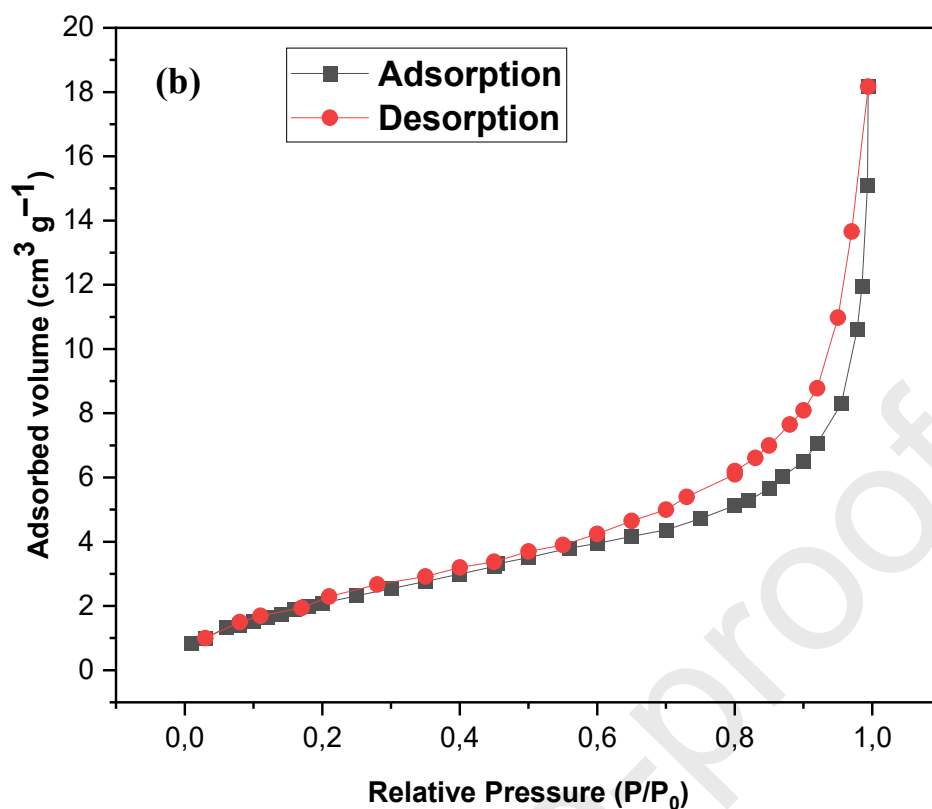


Fig.1. (a) XRD pattern (b) N_2 adsorption–desorption isotherms of nat-HAp before NOR adsorption

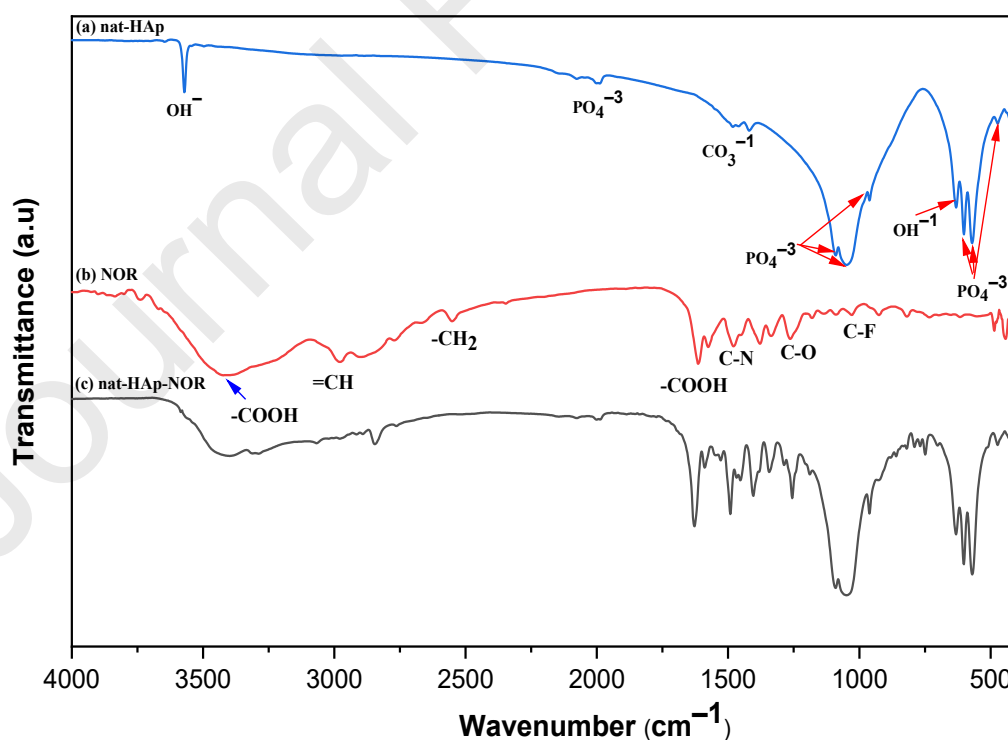
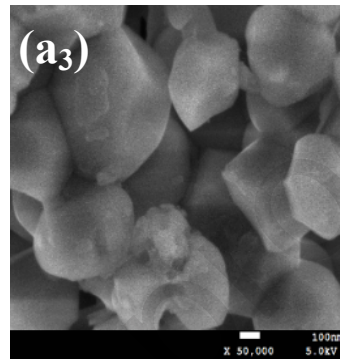
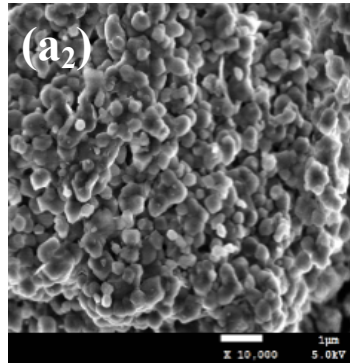
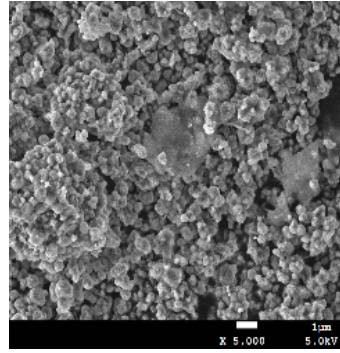
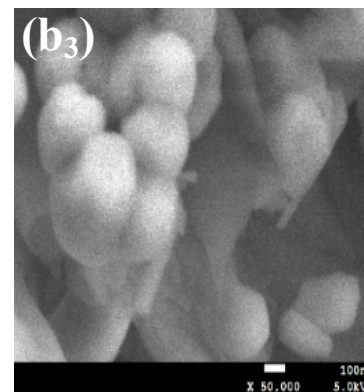
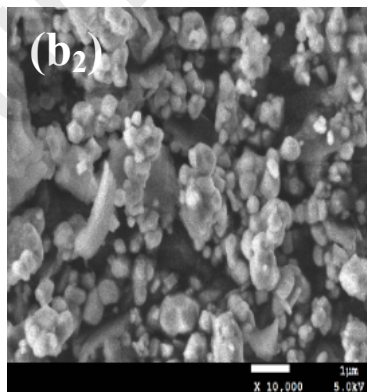
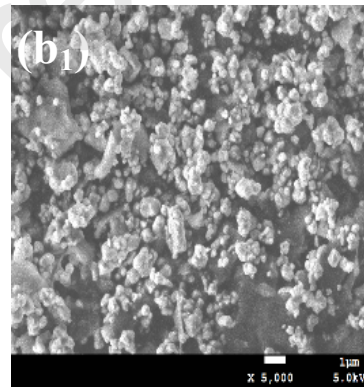


Fig.2. Infrared spectra of (a) nat-HAp ;(b) norfloxacin ;(c) nat-HAp after norfloxacin adsorption (NOR concentration = 200 mg L^{-1} , initial solution pH, nat-HAp dose = 1 g L^{-1} , temperature = $25 \text{ }^\circ\text{C}$, and contact time = 180 min).

(a)



(b)



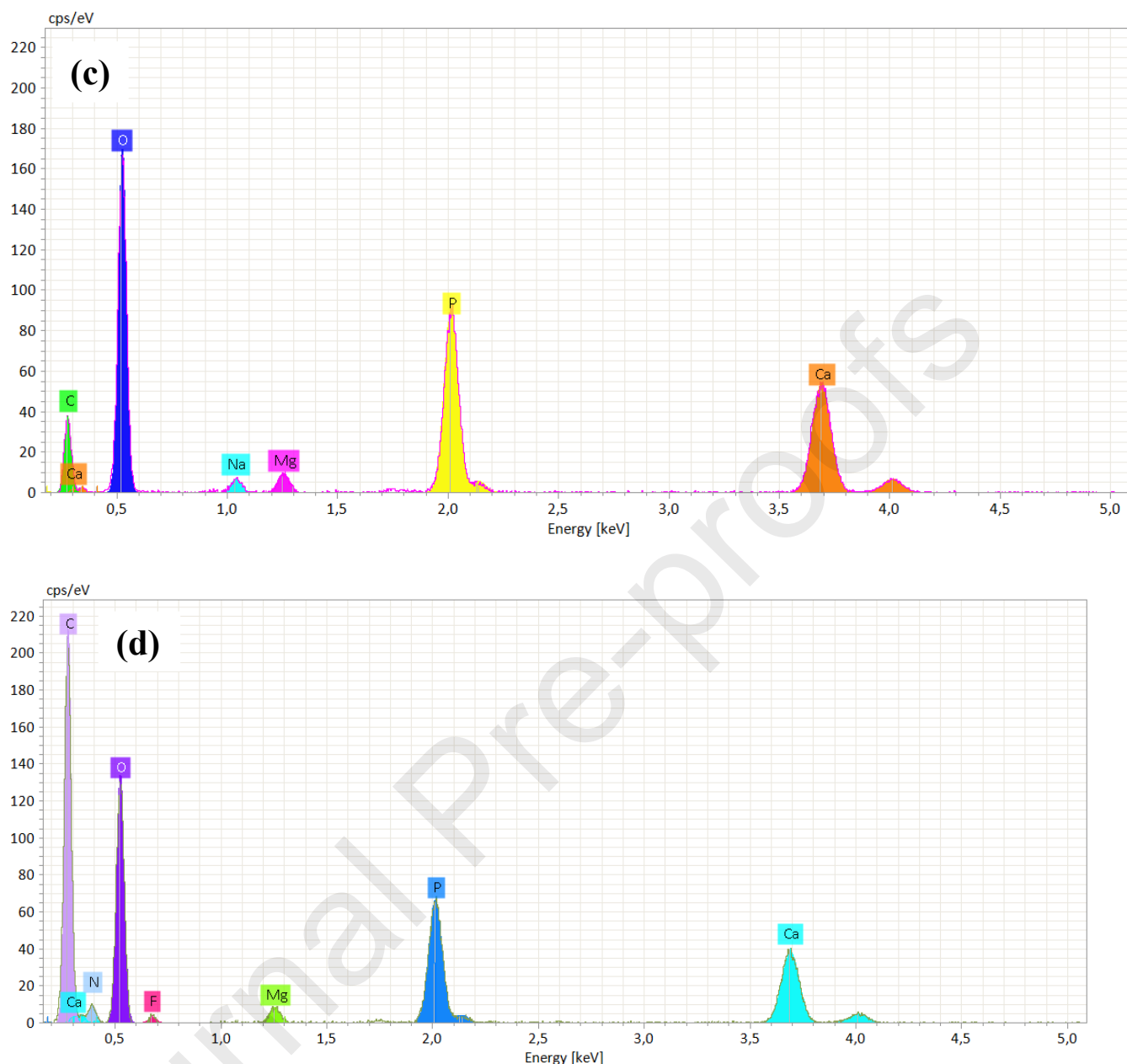


Fig.3. FESEM images of (a) nat-HAP at different magnifications (**a₁**: *5000, **a₂**: *10 000, **a₃**: *50 000) (b) nat-HAP after adsorption at different magnifications (**b₁**: *5000, **b₂**: *10 000, **b₃**: *50 000) (NOR concentration = 200 mg L⁻¹, initial solution pH, nat-HAP dose = 1 g L⁻¹, temperature = 25 °C, and contact time = 180 min); (c) EDX analysis of nat-HAP; (d) EDX analysis of nat-HAP after adsorption (NOR concentration = 200 mg L⁻¹, initial solution pH, nat-HAP dose = 1 g L⁻¹, temperature = 25 °C, and contact time = 180 min).

EDX and FESEM determined our samples' composition and surface morphology. Fig.3 a and b illustrate the FESEM of the nat-HAP powder before and after norfloxacin adsorption, respectively.

FESEM images of the nat-HAP powder (Fig.3a) reveal that the nanoparticles exhibited irregular shapes. However, the morphology of the particles is observed to be nearly irregular hexagonal, with small spheres agglomerated in some regions. It could have been caused by the interaction

of nat-HAp particles [55]. The analysis showed that the product's particle size was approximately 0.1–1 μm . Surface morphological changes of nat-HAp before and after adsorption demonstrate norfloxacin adsorption on nat-HAp.

The values of chemical analysis of the nat-HAp before and after norfloxacin adsorption were obtained using semi-quantitative EDX analysis, presented in Fig. 3c and d, respectively.

EDX spectra confirmed the presence of relevant elements in hydroxyapatite before (Fig. 3c) and after norfloxacin adsorption (Fig. 3d), such as P and Ca. The major constituent is O, with Na, Mg, and C constituting the minor constituents. By loading with NOR, the carbon content of the nat-HAp sample was increased. The presence of N and F peaks in the EDX spectra of norfloxacin-adsorbed hydroxyapatite confirms the norfloxacin adsorption onto nat-HAp, as depicted in Fig. 3d. This result confirms the successful loading of NOR is compatible with previous findings.

3.2. Kinetic studies

Examining adsorption kinetics is critical for treating wastewater because it provides crucial information on the efficiency and nature of the adsorption process.

The pseudo-first-order and pseudo-second-order models [57,58] are used to examine the adsorption capability of an adsorbate on the adsorbent surface. The nonlinear forms of those kinetic models are given as follows:

$$\text{Pseudo-first-order: } q_t = q_e(1 - e^{-k_1 t}) \quad (7)$$

$$\text{Pseudo-second-order: } q_t = \frac{q_e^2 k_2 t}{1 + q_e k_2 t} \quad (8)$$

Where q_t is the adsorption capacity at time t (mg g^{-1}), q_e is the equilibrium adsorption capacity (mg g^{-1}), k_1 is the pseudo-first-order adsorption rate constant (min^{-1}), and k_2 is the pseudo-second-order adsorption rate constant ($\text{g mg}^{-1} \text{min}^{-1}$).

The kinetic models fitted to the experimental data are illustrated in Fig.4. Similarly, the values of the several kinetic parameters in Table 3 were derived using several graphical representations of kinetic equations.

As mentioned in Table 3, R^2 values derived from the pseudo-first-order kinetic model were relatively low. In contrast, the R^2 values derived from the pseudo-second-order model were nearly 1 ($R^2 = 0.999$), indicating that the pseudo-second-order model adequately fits the experimental data. Compared to the pseudo-first-order model, the experimental and calculated q_e values are in close agreement. Hence, the pseudo-second-order model proved effective for modeling the kinetics of NOR adsorption on nat-HAp.

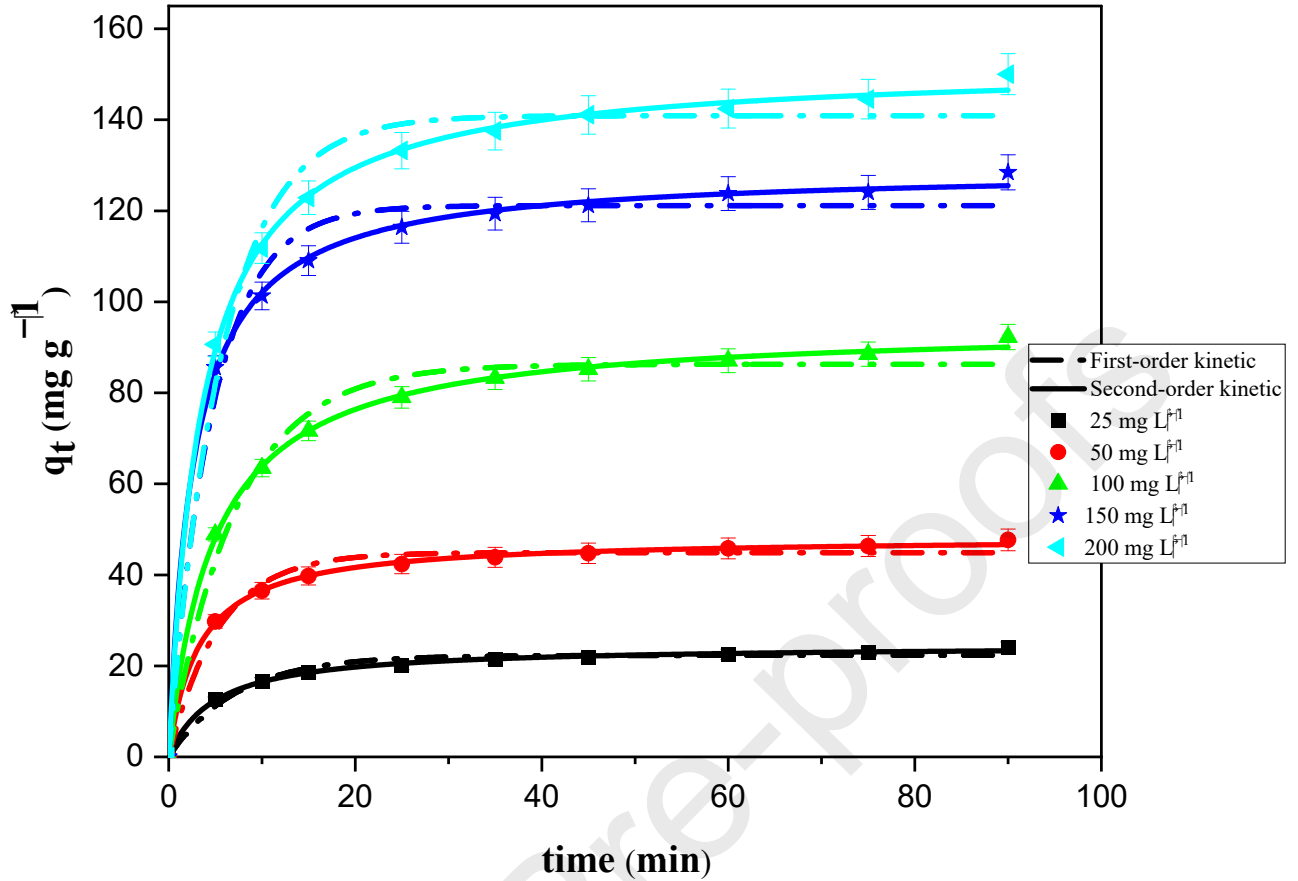


Fig.4. Adsorption kinetics of NOR onto nat-HAp (initial pH = 8, adsorbent dose = 1 g L⁻¹, and temperature = 25 °C)

Table 3. NOR adsorption kinetic parameters onto nat-HAp at different initial concentrations

C ₀ (mg L ⁻¹)	q _{e,exp} (mg g ⁻¹)	Pseudo-first-order kinetic model			Pseudo-second-order kinetic model		
		k ₁ (min ⁻¹)	q _{e,cal} (mg g ⁻¹)	R ²	k ₂ (g mg ⁻¹ min ⁻¹)	q _{e,cal} (mg g ⁻¹)	R ²
25	24.08	0.0013	22.31	0.980	0.0082	24.58	0.998
50	47.48	0.0018	44.89	0.983	0.0064	48.31	0.999
100	92.35	0.0013	86.27	0.983	0.0021	94.91	0.999

150	128.46	0.0021	121.14	0.98	0.0029	129.23	0.999
			4				
200	150.03	0.0017	140.91	0.98	0.0018	152.23	0.999
			3				

3.3. Adsorption isotherms

The adsorption isotherm is a fundamental theoretical basis for the practical application of adsorption, which is characterized by constants whose values indicate the surface characteristics and affinity of the sorbent sorption equilibrium [59].

Various mathematical models are given for experimental adsorption values, with Langmuir, Freundlich, and Temkin isotherms being the most often utilized. In the present work, these models were utilized to depict the interactions between NOR molecules and the nat-HAP surface and examine NOR distribution in the solid and liquid phases. Adsorption process optimization requires finding the optimal isotherm model. The equations below represent the nonlinear equations of those isotherm models [57,58]:

$$\text{Langmuir isotherm: } q_e = \frac{q_m K_L C_e}{1 + K_L C_e} \quad (9)$$

$$\text{Freundlich isotherm: } q_e = K_F C_e^{1/n_F} \quad (10)$$

$$\text{Temkin isotherm: } q_e = \left(\frac{RT}{b_T}\right) \text{Ln}(K_T C_e) \quad (11)$$

Where C_e and q_e are the NOR concentration (mg L^{-1}) and equilibrium adsorption capacity (mg g^{-1}) at equilibrium, respectively; q_m is the maximum adsorption capacity of adsorbents (mg g^{-1}); and K_L represent the Langmuir adsorption constant (L mg^{-1}), K_F is the Freundlich adsorbent capacity ($\text{mg g}^{-1}(\text{L mg}^{-1})^{(1/n_F)}$), n_F is the heterogeneity factor, K_T is the Temkin equilibrium binding constant (L mg^{-1}), and b_T is the Temkin constant (J mol^{-1}). The plots of these isotherm models are displayed in Fig.5, and their coefficients are listed in Table 4.

The Langmuir isotherm can be described in terms of the dimensionless constant separation factor, R_L , as given by the following equation:

$$R_L = \frac{1}{1 + K_L C_0} \quad (12)$$

Where K_L is the Langmuir constant (L mg^{-1}), and C_0 is the initial NOR concentration (mg L^{-1}).

The R_L parameter indicates the shape of the isotherm to be either unfavorable ($R_L > 1$), linear ($R_L = 1$), favorable ($0 < R_L < 1$), or irreversible ($R_L = 0$) [60]. Calculated values at different NOR concentrations indicate that $0.029 \leq R_L \leq 0.19$, a result showing favorable adsorption.

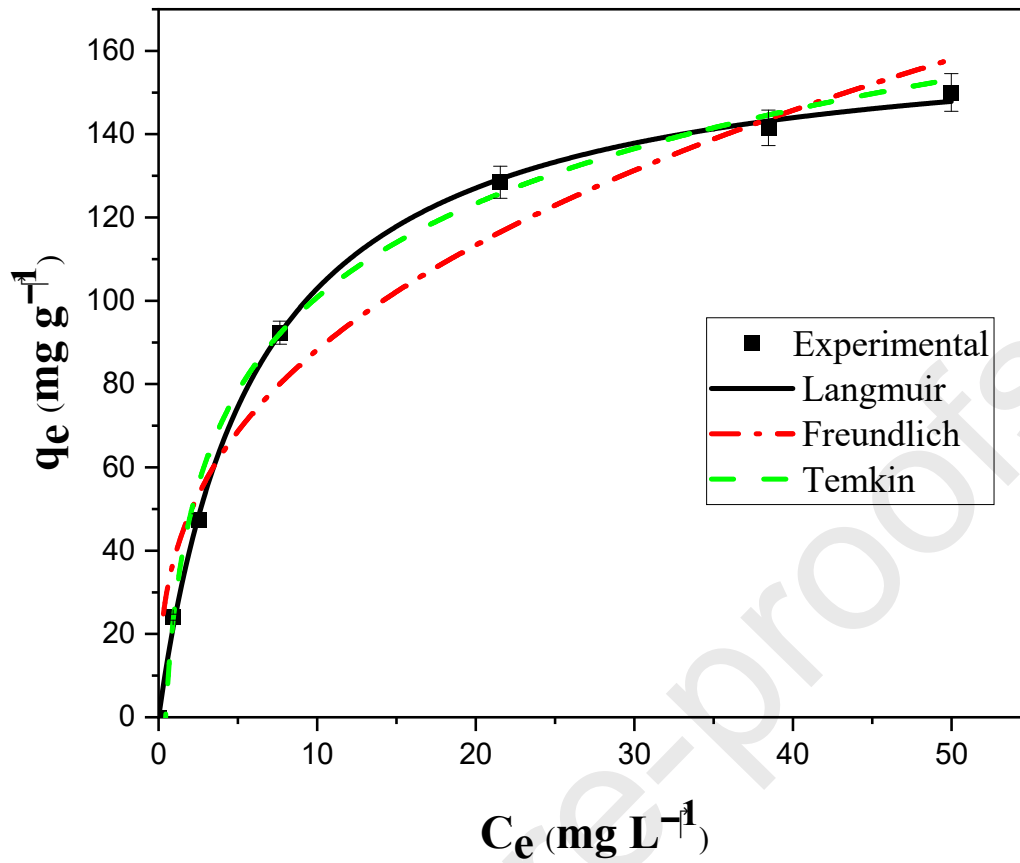


Fig. 5. Adsorption isotherms of Norfloxacin onto nat-HAp (initial pH = 8, adsorbent dose = 1 g L⁻¹, and temperature = 25 °C).

Table 4. NOR adsorption Isotherm parameters on nat-HAp

Isotherm	Parameters	Values
Langmuir	q_m (mg g ⁻¹)	166.01
	K_L (L mg ⁻¹)	0.1632
	R^2	0.999
	R_L	0.1970
Freundlich	K_F (mg g ⁻¹ (L mg ⁻¹) ^(1/n_F))	38.3627
	n_F	2.7637

	R^2	0.974
Temkin	K_T (L mg ⁻¹)	2.0692
	b_T (J mol ⁻¹)	75.8363
	R^2	0.996

Compared to the other isotherm models, the Langmuir model offered the best fit to the experimental data with the highest regression coefficient ($R^2 = 0.999$).

This data indicates that NOR is adsorbed onto the surface of nat-HAp through monolayer adsorption. A favorable adsorption process is indicated by the R_L value of 0.197. The Temkin model's correlation coefficient was equally excellent ($R^2 = 0.996$), which indicates good representativity.

3.4. Comparison of adsorption capacity of nat-HAp with other adsorbents

Various adsorbents with distinct structures and chemical compositions have been developed to remove the NOR antibiotic from aqueous solutions. Therefore, it would be beneficial to compare nat-HAp to other adsorbents used for the adsorption of NOR. According to Table 5, nat-HAp presented a higher q_m value than other reported adsorbents. The high q_m of nat-HAp may be attributable to specific functional groups and charge properties of the surface, such as the strong electrostatic contact between the anionic NOR antibiotic and the positive charge surface of nat-HAp.

Table 5. Comparison of equilibrium time and q_m of nat-HAp with other adsorbents for NOR adsorption.

Adsorbent	Equilibrium Time (h)	q_m	References
		(mg g ⁻¹)	
Manganese oxide-loaded magnetic Biochar (MMB)	4	6.94	[61]
ZIF-8-Derived Hollow Carbon(ZHC)	20	125.6	[62]
Zr-based metal-organic frameworks (UiO-66-NH ₂)	6	222.2	[63]
Pomelo peel biochar loaded with γ -Fe ₂ O ₃ (γ -Fe ₂ O ₃ @BC)	3	85.08	[13]

Iron ore waste (IOW)	72	8.64	[7]
Sodium Alginate/Modified Bentonite Composite (GOMBt)	24	3.84	[64]
Natural colemanite	24	3.43	[65]
nat-HAp	3	166.01	Present work

3.5. Response surface modeling

3.5.1. Experimental design and quadratic model

BBD was used to optimize the significant variables. Table 6 presented design matrix and results of 27 BBD-analyzed tests. The regression equation achieved after ANOVA gives the NOR antibiotic removal efficiency onto nat-HAp as a function of several factors, such as antibiotic concentration (A), pH (B), adsorbent dosage (C), and temperature (D). All terms of factors were included in the equation given below:

$$Y (\text{removal efficiency, \%}) = 73.70 - 4.86 \times A + 11.98 \times B + 12.18 \times C - 10.88 \times D + 1.95 \times AB + 0.39 \times AC + 0.45 \times AD - 15.49 \times BC + 5.84 \times BD + 3.30 \times CD - 4.93 \times A^2 - 10.05 \times B^2 - 1.17 \times C^2 - 3.28 \times D^2 \quad (13)$$

A, *B*, *C*, and *D* are independent singular variables in the preceding equation, whereas *AB*, *AC*, *AD*, *BC*, *BD*, and *CD* are interaction factors. The quadratic terms are A^2 , B^2 , C^2 , and D^2 .

Table 6. BBD matrix for four variables together with the observed response

Run order	NOR (A)	pH(B)	Dose(C)	T(D)	Y (%)	Y (%)
-----------	---------	-------	---------	------	-------	-------

27 100 8 1.00 40 83.00 84.24

Contact time and stirring speed were constant at 180 min and 200 rpm, respectively

The Box–Behnken responses were analyzed, and the results of ANOVA for the adsorption study of Norfloxacin are presented in Table 7.

Table 7. ANOVA, regression coefficient estimates, and significance test for norfloxacin absorption on nat-HAp

Source	Sum Squares	of	df	Mean Square	F-value	p-value
Model	6960.27		14	497.16	159.18	< 0.0001 significant
A-Initial concentration	283.44	1	1	283.44	90.75	< 0.0001
B-pH	1722.72	1	1	1722.72	551.57	< 0.0001
C-Adsorbent dose	1780.23	1	1	1780.23	569.98	< 0.0001
D-Temperature	1421.36	1	1	1421.36	455.08	< 0.0001
AB	15.17	1	1	15.17	4.86	0.0478
AC	0.6320	1	1	0.6320	0.2024	0.6608
AD	0.8281	1	1	0.8281	0.2651	0.6160

BC	959.76	1	959.76	307.29	< 0.0001	
BD	136.31	1	136.31	43.64	< 0.0001	
CD	43.63	1	43.63	13.97	0.0028	
A ²	129.63	1	129.63	41.50	< 0.0001	
B ²	538.68	1	538.68	172.47	< 0.0001	
C ²	7.27	1	7.27	2.33	0.1530	
D ²	57.47	1	57.47	18.40	0.0011	
Residual	37.48		123.12			
Lack of Fit	20.91		102.09	0.2523	0.9460	not significant
Pure Error	16.57	2	8.29			
Cor total	6997.75		26			

$R^2 = 0.9946$; $R_{adj}^2 = 0.9884$; $R_{pred}^2 = 0.9775$; *df*: Degrees of freedom; *A* (Initial concentration), *B* (pH), *C* (Adsorbent dose), and *D* (temperature).

ANOVA was performed to examine the model's significance and fitness. The model *F-value* is the ratio of the individual term's mean square to the residual term's mean square. The model *F-value* of 159.18 indicates that the model is significant.

The P-values were utilized to determine the significance of each coefficient [43], which may show the interaction pattern between the factors. This analysis demonstrates that the coefficients *A*, *B*, *C*, *D*, *AB*, *BC*, *BD*, *CD*, *A*², *B*², and *D*² were statistically significant with very small p-values ($p < 0.05$). The other variables' coefficients were insignificant ($p > 0.05$). An *F-value* of 0.25 indicates that the lack of fit is not statistically significant compared to the pure error. Indeed, a non-significant lack of fit is desired, because we want the model to fit.

In addition, the coefficient of determination (R^2) and the adjusted coefficient of determination (R_{adj}^2) were used to verify the validity of the model.

In the present model, the R^2 and adjusted R^2 values are 0.9946 and 0.9884, respectively, corresponding well to the respective experimentally obtained values. The R^2 value of 0.9946 shows that the model accounted for 99% of the variance in norfloxacin adsorption, whereas 1% was attributed to residual variation. In addition, a closely high adjusted correlation coefficient value indicated the model's high significance [66].

In this study, a ratio of 15.066 is determined, indicating the dependability of the experiment results. The degree of precision is shown by the standard deviation $SD = 1.77$ and coefficient of variation $CV = 2.72$. The low values of SD and CV indicate that the experiment is executed appropriately. The models exhibit a high R^2 value, a significant F -value, a not significant p -value for lack of fit, and a low standard deviation and variance coefficient. These results demonstrate the accuracy with which norfloxacin removal efficiency by nat-HAp may be predicted. Consequently, the models were utilized for additional study.

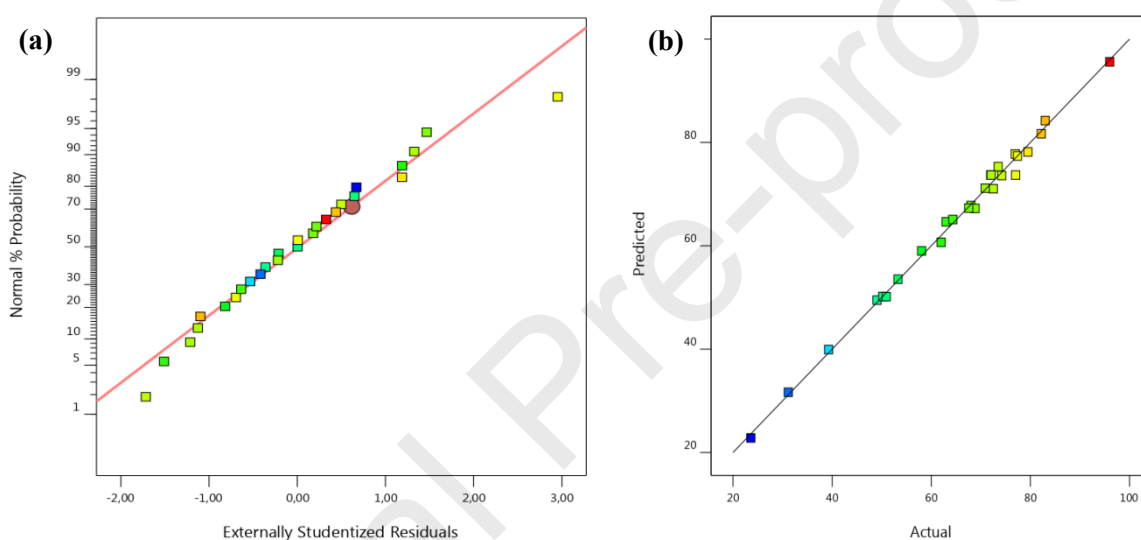
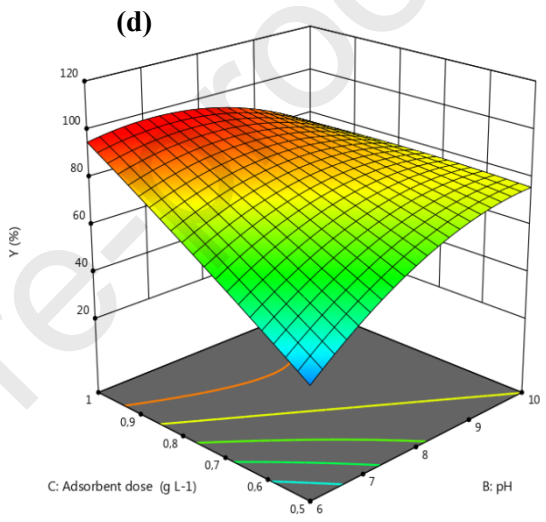
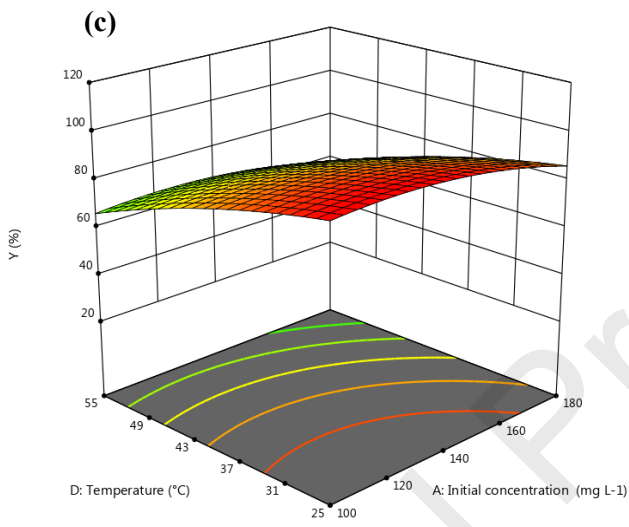
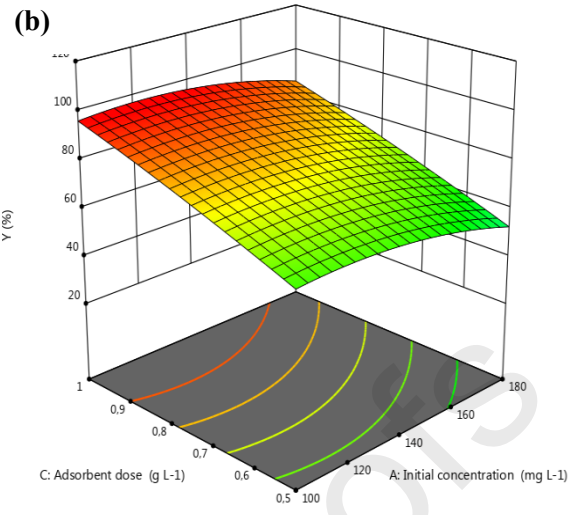
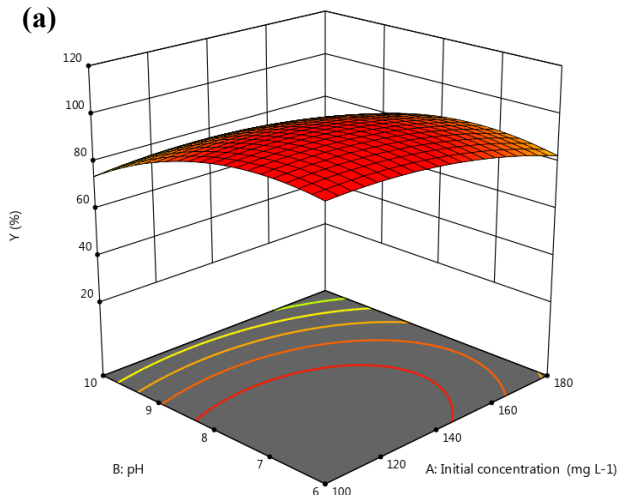


Fig. 6. (a) Normal % probability versus residual error; (b) predicted response versus actual response.

The data were also evaluated to determine the residuals' normality. Fig.6a depicts a normal probability map of these residuals. This graph's data points are near a straight line. The relationship between the expected and actual values of Y for the adsorption of Norfloxacin onto nat-HAp is depicted in Fig. 6b.

Fig. 6b illustrates that the developed model is adequate because the residuals for most predicted responses are less than 10% and tend to be near the diagonal line.



(e)

(f)

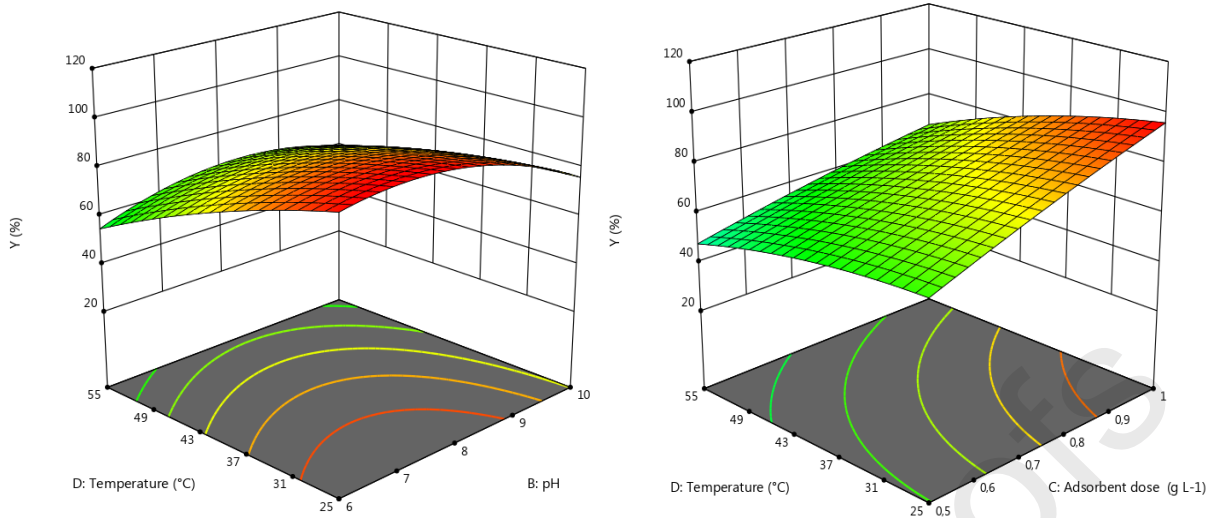


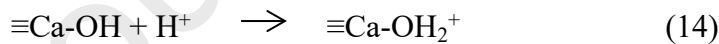
Fig.7. Response surface plots for norfloxacin removal efficiency (%) onto nat-HAP showing the interaction between (a) initial solution pH and NOR concentration, (b) nat-HAP dose and NOR concentration, (c) temperature and NOR concentration, (d) nat-HAP dose and initial solution pH, (e) temperature and initial solution pH (f) temperature and nat-HAP dose.

3.5.2. Effect of operating parameters and binding mechanism

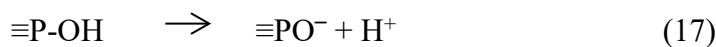
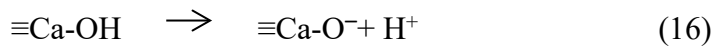
The BBD and RSM were used to determine out how four key factors affected the procedure for adsorbing Norfloxacin. The pH solution is a crucial control factor because it influences the surface charge of the adsorbent and the ionic speciation of adsorbate molecules [67]. The distribution of NOR species at various pH levels is depicted in Fig.8b. Therefore, NOR occurs in three ionization states: cationic (NOR⁺) at pH < 6.22, zwitterionic (NOR[±]) at 6.22 < pH < 8.51, and anionic (NOR⁻) at pH > 8.51[68].

The surface charge of nat-HAP was examined throughout a broad pH range, ranging from 3 to 12. Based on the inset of Fig.8a, the pHz_{PC} value of nat-HAP was basic (pHz_{PC} = 10.5) because the concentration of primary sites was greater than that of acid sites [69]. The functional groups influencing the surface charge of nat-HAP are the hydroxyls, ≡Ca-OH, and the P-OH phosphates [34].

The surface of nat-HAP was positively charged as a result of the ensuing protonation processes:



In contrast, the negative charge on the surface of nat-HAP was generated through the ensuing deprotonation processes:

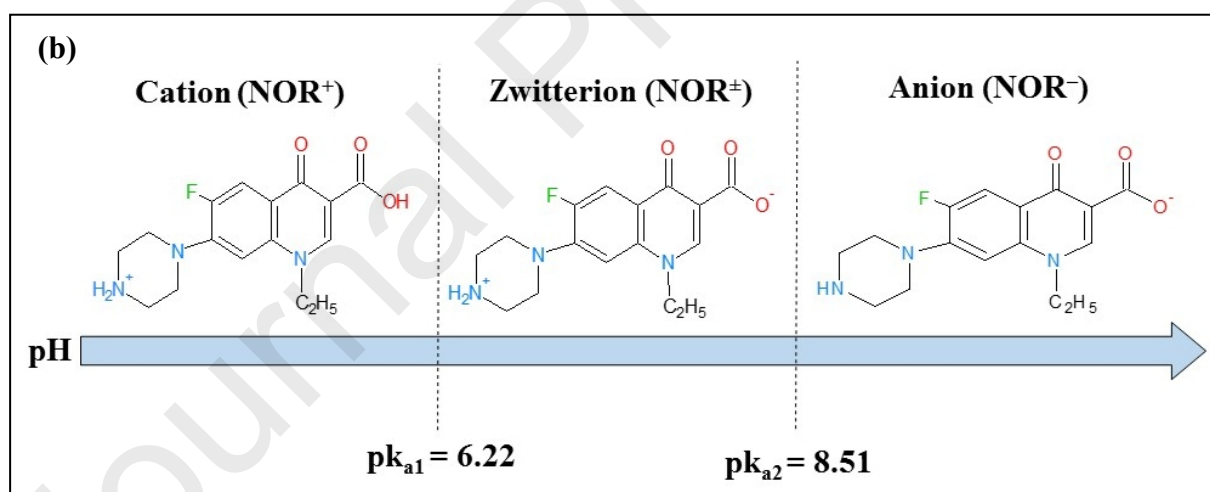
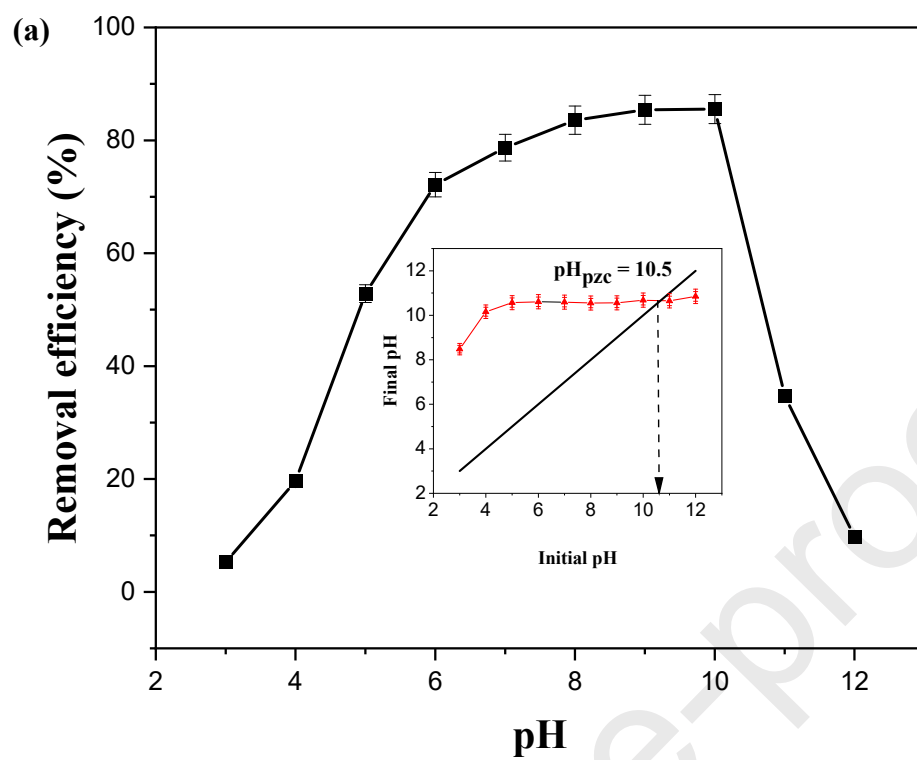


where ≡ indicates the surface of nat-HAP. Thus, protonation processes prevailed at pH < pHz_{PC}, but deprotonation reactions occurred at pH > pHz_{PC}. At pH levels close to pHz_{PC}, the nat-HAP surface establishes an equilibrium between anionic and cationic active sites.

At pH levels ranging from 3 to 12, the effect of pH on NOR elimination by nat-HAp was studied. As shown in Fig.8a, NOR removal increased from 5.32 to 72.17 %, when pH increased from 2.0 to 6.0. The electrostatic repulsions between NOR^+ and the positively charged nat-HAp surface ($\equiv\text{CaOH}_2^+$ and $\equiv\text{POH}$) are responsible for the observed norfloxacin adsorption pattern. Fig.7a, d, and e, respectively, depict the interaction between pH, initial concentration, adsorbent dose, and temperature ranges between 6 and 10 were more favorable for norfloxacin adsorption (close to the pH_{ZPC} value of nat-HAp, where $\equiv\text{PO}^-$, and $\equiv\text{CaOH}_2^+$ groups predominate) [67,68]. The NOR^+ cationic form transforms into the NOR^\pm zwitterion form within this pH range. Thus, the $\equiv\text{PO}^-$, and $\equiv\text{CaOH}_2^+$ surface sites of nat-HAp are electrostatically attracted to $> \text{NH}_2^+$ and $-\text{COO}^-$ groups of NOR^\pm , respectively. In addition, zwitterionic NOR^\pm was more hydrophobic than its cationic and anionic forms [63]. In addition to hydrophobic and electrostatic interactions, we hypothesize that the creation of hydrogen bonds is a crucial element of the adsorption process of the polar organic molecule norfloxacin [70].

NOR's carbonyl and hydroxyl groups tend to form H-bonding dipole–dipole interactions with oxygen atoms on the surface of nat-HAp. The hydrogens of the hydroxyl and amine groups of NOR functioned as H-bond donors. In contrast, the nitrogen-, oxygen- and fluorine-containing polar NOR groups can function as H-bond acceptors. The benzene ring of NOR also acted as an H-bond acceptor when Yoshida H-bonds were created with the hydroxyl groups of the nat-HAp adsorbent. Oxygen-containing nat-HAp's functional groups (P-OH and Ca-OH) are essential for their high affinity for NOR molecules.

Various H-bond forming pathways between NOR and nat-HAp were anticipated to play a crucial role in adsorption affinity. The $n-p$ electron interactions between the oxygenated groups of the nat-HAp (as n -donor) and the aromatic ring of NOR (as π -receptor) may be another factor in the mechanism of NOR binding. Similar arguments have been presented for NOR adsorption on pomelo peel biochar loaded with $\gamma\text{-Fe}_2\text{O}_3$ [70]. In light of the above discussion, the proposed NOR binding mechanism on the nat-HAp surface is portrayed in Fig. 8(c).



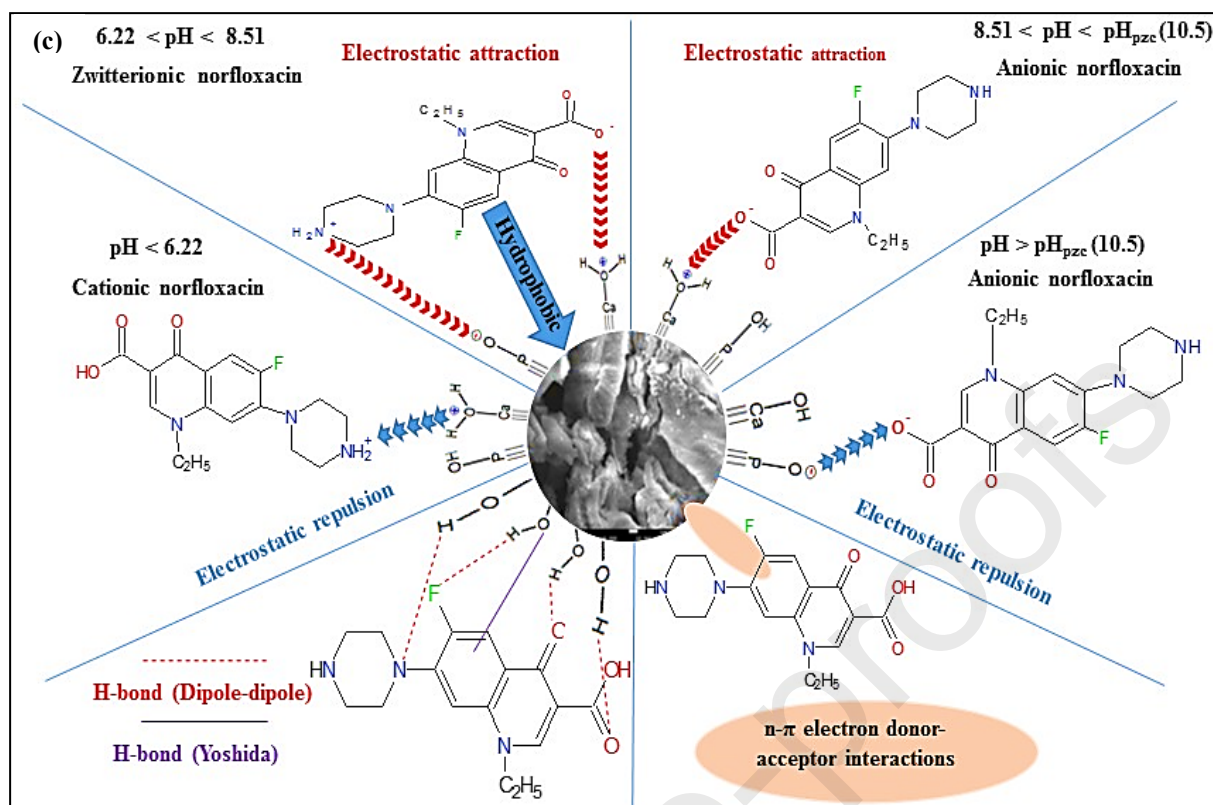


Fig. 8. (a) pH effect on NOR adsorption by nat-HAp (Inset: pH_{ZPC} determination of nat-HAp) (NOR concentration = 150 mg L^{-1} , nat-HAp dose = 1 g L^{-1} , temperature = $25 \text{ }^\circ\text{C}$, and contact time = 180 min) (b) predominance diagram of NOR (c) proposed binding mechanism of the NOR antibiotic on the nat-HAp.

Another impactful parameter in the adsorption process is the dose of adsorbent, which defines the capacity of the adsorbent to eliminate the contaminant species at a particular initial concentration. Fig. 7b, d, and f, respectively, illustrate the interaction between adsorbent dose, initial concentration, initial pH, and temperature. It demonstrates that the removal effectiveness increased as the adsorbent dosage increased from 0.5 g L^{-1} to 1 g L^{-1} , which could be attributed to the greater availability of sorptive sites on the surface of the sorbent. Somewhat similar observations were reported by Imessaoudene et al.[40]. The norfloxacin adsorption onto nat-HAp was performed at concentration between 100 and 180 mg L^{-1} .

Fig. 7a, b, and c show the influence of initial concentration on adsorption while maintaining two constant parameters. According to the response graphs, NOR's Y (%) decreases with increasing initial concentration up to 100 – 180 mg L^{-1} . This trend may be due to the fixed number of active sites on the adsorbent vis-à-vis an increasing number of NOR molecules [71].

In Fig. 7b, d, and e, the response surface plots reveal that NOR Y (%) increased when temperature decreased from 50 to 25°C , indicating that the adsorption process was exothermic, which we will confirm hereafter by the thermodynamic study.

3.6. Thermodynamics studies

Thermodynamics data provide information on the feasibility of a sorption process. Adsorption experiments were conducted between 25 and 55 °C. Fig.7c, e, and f illustrate the influence of temperature on NOR removal when two factors are held constant. These figures demonstrate that the elimination of NOR reduces with increasing temperature. The reduction in NOR removal with increasing temperature suggests that Norfloxacin is positively adsorbed by nat-HAp at lower temperatures, indicating that the adsorption process is exothermic.

Using Equation (9), the Langmuir isotherm constant (K_L) was utilized to calculate the thermodynamic equilibrium constant K_e° for nat-HAp at various temperatures (25–55 °C) because this isotherm model provided the best fit for the experimental equilibrium data [72,73].

$$K_e^\circ = \frac{1000 K_L M_{adsorbate} [Adsorbate]^\circ}{\gamma} \quad (18)$$

where $M_{adsorbate}$ (319.33g mol⁻¹) is the atomic mass of NOR; $[Adsorbate]^\circ$ (1 mol L⁻¹) is the standard concentration of adsorbate; γ is the coefficient of activity of the NOR antibiotic solution as unitary for infinite dilution. To calculate ΔG° (standard Gibbs energy change), Equations (19) and (20) are used:

$$\Delta G^\circ = -RT \ln K_e^\circ \quad (19)$$

$$\Delta G^\circ = \Delta H^\circ - T\Delta S^\circ \quad (20)$$

where T (K) is the temperature; R (8.314 J K⁻¹ mol⁻¹) is the universal gas constant. The combination of Equations (19) and (20) has resulted in Equation (21):

$$\ln K_e^\circ = \frac{\Delta S^\circ}{R} - \frac{\Delta H^\circ}{RT} \quad (21)$$

The plot of $\ln K_e^\circ$ vs. $1/T$ produced a straight line (Fig.9) and from the intercept and slope of these van't Hoff plots, the values of ΔH° (kJ mol⁻¹) and ΔS° (J mol⁻¹K⁻¹) may be derived, respectively. Table 8 displays the thermodynamic values calculated NOR of 150 mg L⁻¹, nat-HAp of 1 g L⁻¹, and pH of 7.88

Table 8. Thermodynamic parameters for adsorption of NOR onto nat-HAp

T (K)	K_L (L mg ⁻¹)	$\ln K_e^\circ$	ΔG° (kJ mol ⁻¹)	ΔH° (kJ mol ⁻¹)	ΔS° (J mol ⁻¹ K ⁻¹)
298	0.1632	10.86	-26.91	-37.44	-35.34
308	0.1025	10.39	-26.55		
318	0.0602	9.86	-26.20		

328 0.0420 9.50 -25.85

The negative values of ΔG° showed a spontaneous removal process. In addition, the increasing negative value of ΔG° as the temperature rises indicates that the removal process is advantageous at lower temperatures. Observe that the value of K_L decreases with increasing temperature, and the value of ΔH° is negative; this confirms that the adsorption is exothermic, which is consistent with the study of the adsorption of NOR onto Mg-Al double hydroxides [74]. The value of ΔH° was $< 80 \text{ kJ mol}^{-1}$, indicating the formation of weak bonds (physisorption) between NOR and nat-HAp [50]. This is consistent with the suggested adsorption mechanism.

In addition, a negative change in entropy ΔS° implies that the elimination process is driven by enthalpy. During the adsorption phase, it also shows a loss of randomization at the interface between the adsorbent and antibiotic solution, which results in the escape of adsorbate molecules from the solid phase into the liquid media and explains the drop in removal effectiveness with rising solution temperature [75].

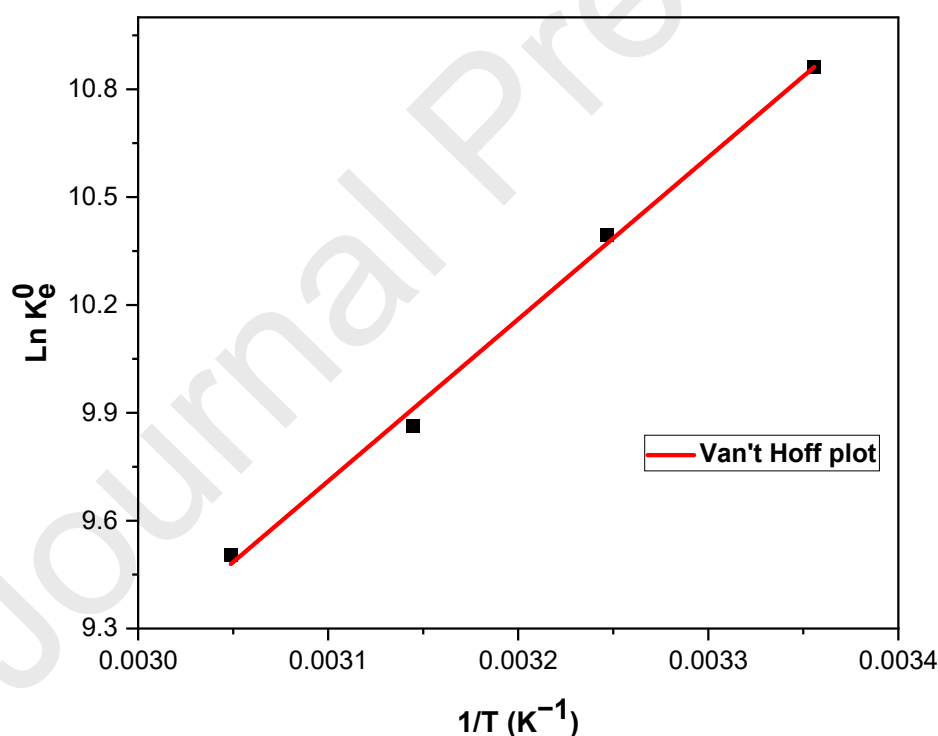


Fig.9. Van't Hoff plot for NOR adsorption on the nat-HAp material

3.7. Optimization using the desirability function and model validation

Mathematical optimization can give each input factor and response a suitable value. Optional input optimizations include the minimum, maximum, target, range, and none (for responses) and determining the optimal output for a given set of conditions [76].

In this study, the input variables were assigned predefined ranges of values, while the response was intended to reach its maximum value. Under these conditions, the most excellent norfloxacin removal efficiency attained was 96.20 % (Fig.10) at an initial pH of 7.88, a norfloxacin concentration of 138.57 mg L⁻¹, an adsorbent dose of 1 g L⁻¹, and a temperature of 25.06 °C.

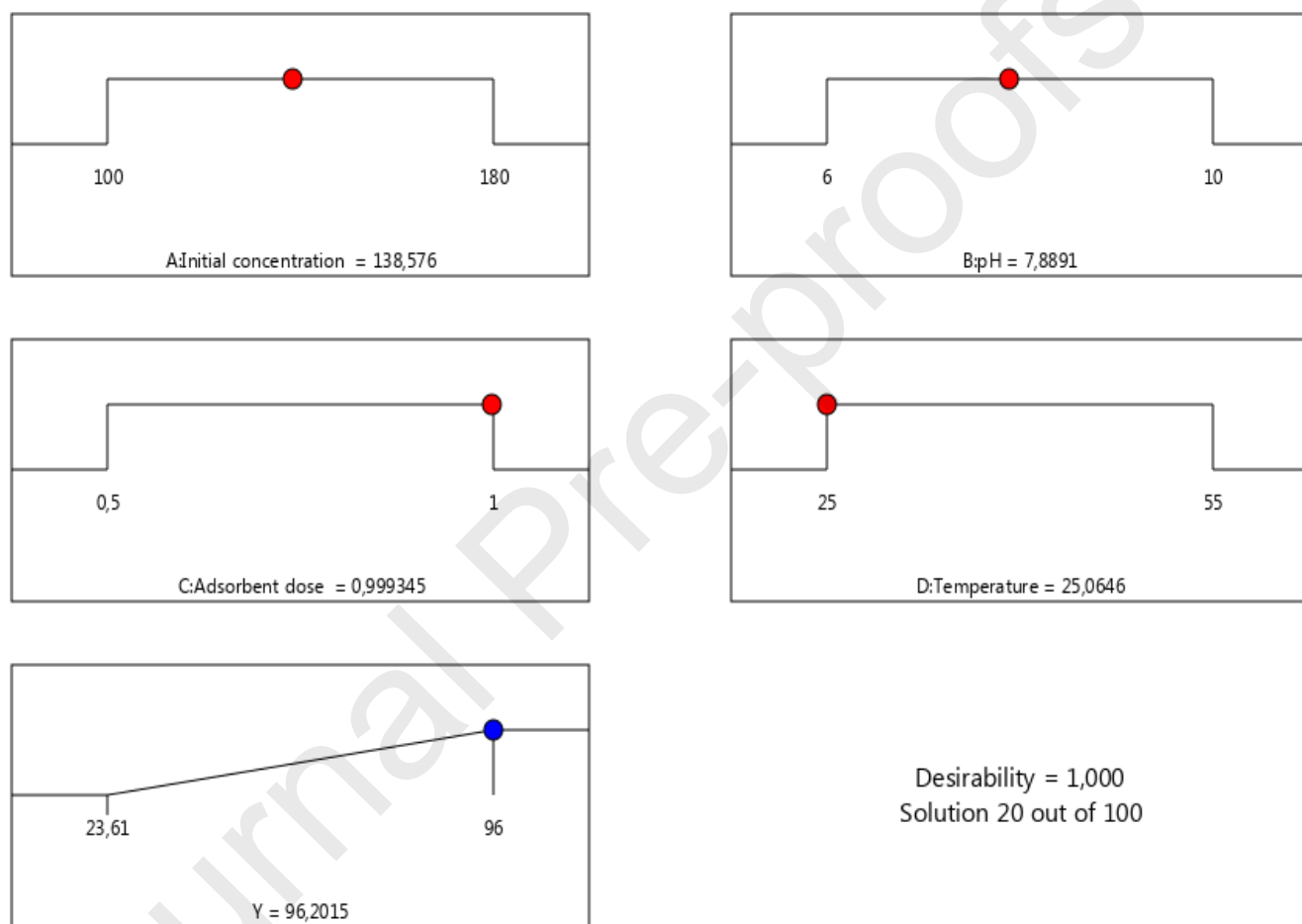


Fig.10. Desirability ramp for optimization.

Experiments were conducted for a specific optimum medium configuration to validate the mathematical model created by RSM implementation. In order to validate the actual value, the experiment was based on these appropriate conditions. The laboratory findings yielded a value of 95.45%, which was quite near the optimal value obtained using RSM tools and fit well.

3.8. Desorption experiments

The results indicate that desorption efficiency found at pH 3, 5.5, 8.5, and 12, around 98.52%, 64.86%, 34.45%, and 45.78%, respectively.

Under extreme pH conditions ($\text{pH} = 3$ and $\text{pH} = 12$), when the surfaces of the adsorbent and NOR molecules have identical positive charges, adherent adsorbate molecules can desorb due to electrostatic repulsion [39,77]. In addition, the conspicuous presence of protons at low pH levels can result in the exchange of protons with positively charged NOR molecules adsorbed on the adsorbent surface, releasing the adsorbed NOR molecules. Observing a modest increase in pH value further support this hypothesis. The increase in NOR concentration in solution with decreased pH suggests that most antibiotic adsorption was mediated by electrostatic attraction [78]. As desorption cycles increased, the regenerated adsorbent's adsorption effectiveness declined [79]. At $\text{pH} = 3$, after four repeated cycles (Fig.11), the Y (%) of nat-HAp was found to be 64.10 %.

The nat-HAp is readily regenerated by altering the solution's pH. nat-HAp has considerable promise as a reusable antibiotic adsorbent that is difficult to renew, such as activated carbon [80].

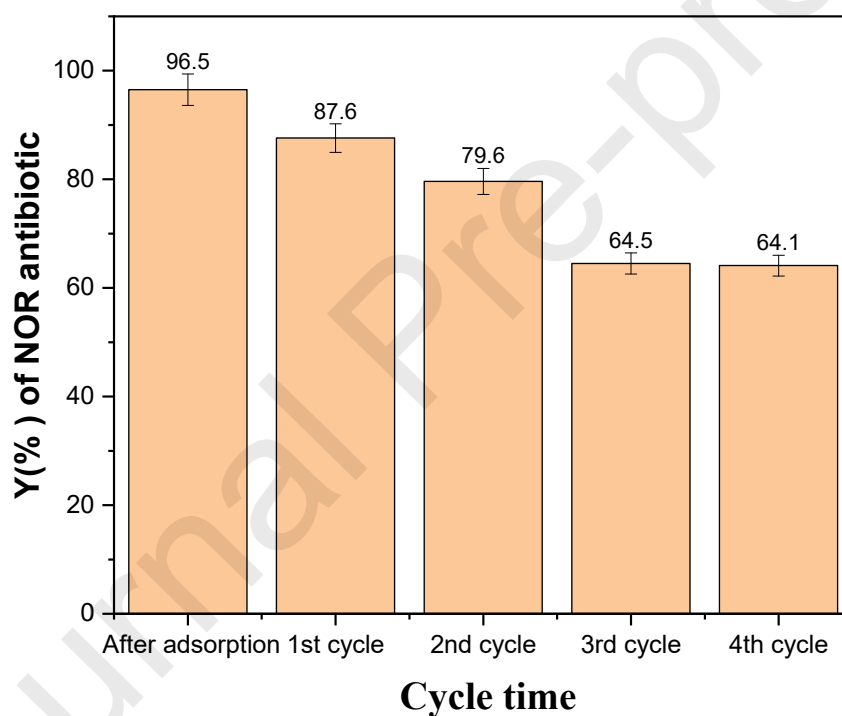


Fig. 11. Desorption cycles for NOR antibiotic using nat-HAp at $\text{pH} = 3$

3.9. Estimation of preparation cost for Nat-HAp

Energy and Cost Estimate is a thoughtful forecast of the likely cost of manufacturing that proposes a precise budget for the material used. The entire energy and cost required in this study to manufacture roughly 1 kg of nat-HAp was estimated and listed in Table 9.

Table 9. Energy and cost estimation for the preparation of 1 kg of nat-HAp.

	Factor	nat-HAp
Bovine bone preparation (Pre-treatment , drying and grinding)	Cost (\$USD/1kg)	0.07
	Power (W)	2500
Calcination process (pyrolyzing)	Time consumed (min)	180
	Total cost (\$USD/25.0 g)	0.25
	Total cost (\$USD/1kg)	10.07

*Algeria tariff rates of electricity, 0.034 \$USD/kWh.

The cost for producing nat-HAp was estimated mainly based on the cost related to energy consumption (mainly including the bones pre-treatment, grinding, drying, and pyrolyzing costs) was 10.07 \$USD/kg. Pyrolyzing of bovine bone leads to a potential cost-effective adsorbent for removing fluoroquinolone antibiotics from industrial wastewater, contributing to low-energy and low-cost consumption for a green sustainability.

4. Conclusion

This work studied the adsorption of NOR from aqueous solutions using natural hydroxyapatite derived from bovine bone by calcination at 800 °C. Response surface methodology was utilized to maximize the removal of norfloxacin by the nat-HAp adsorbent. Experiments were conducted using a statistical design based on the Box–Behnken surface with four input variables: initial concentration, pH, adsorbent dose, and temperature. Contact time (180 min) was considered a constant input parameter. With a coefficient of determination (R^2) of 0.994 and an F -value of 159.18, the second-order polynomial regression model was likewise found to characterize the experimental data adequately. Using the desirability function approach, the optimal parameters were an initial concentration = 138.57 mg L⁻¹, initial pH = 7.88, adsorbent dose = 0.99 g L⁻¹, and temperature = 25.6 °C, which resulted in a maximum norfloxacin removal of 96.20% and desirability of 1. The Langmuir model provided the best-fitting adsorption isotherm, showing that adsorption occurs via monolayer coverage. The adsorption process is exothermic, as demonstrated by the negative enthalpy change. The kinetic studies indicated that the adsorption fitted the pseudo-second-order model.

Hydrophobic interactions, electrostatic forces, n - π electron donor–acceptor interactions, and H-bonding primarily involved NOR adsorption mechanism over the nat-HAp. Desorption studies demonstrated that the adsorbent nat-HAp could be regenerated after four cycling runs with a removal efficiency of 64.10 %. Due to the low cost and abundance of nat-HAp, this material is auspicious for removing fluoroquinolone antibiotics from industrial wastewater.

Acknowledgments

The authors wish to thank all who assisted in conducting this work.

Data availability statement

The authors confirm that the data supporting the findings of this study are available within the article [and/or] its supplementary materials.

Disclosure statement

The authors report that there are no competing interests to declare.

References

- [1] H. Fu, X. Li, J. Wang, P. Lin, C. Chen, X. Zhang, M. Suffet, Activated carbon adsorption of quinolone antibiotics in water: Performance, mechanism, and modeling, *J. Environ. Sci.* 56 (2016). <https://doi.org/10.1016/j.jes.2016.09.010>.
- [2] W. Song, Pollution Characteristics and Risk Assessment of Typical Antibiotics and Persistent Organic Pollutants in Reservoir Water Sources, *Water*. 15 (2023) 259. <https://doi.org/10.3390/w15020259>.
- [3] M. Jalil, M. Baschini, K. Sapag, Removal of Ciprofloxacin from Aqueous Solutions Using Pillared Clays, *Materials*. 10 (2017) 1345. <https://doi.org/10.3390/ma10121345>.
- [4] Y. Cheng, T. Ding, Y. Qian, M. Li, J. Li, Advances in biodegradation of pharmaceuticals and personal care products, *Sheng Wu Gong Cheng Xue Bao Chin. J. Biotechnol.* 35 (2019) 2151–2164. <https://doi.org/10.13345/j.cjb.190191>.
- [5] G. Marc, C. Araniciu, S. Oniga, L. Vlase, A. Pirnau, G. Nadăș, C. Novac, I. Matei, M. Chifiriuc, L. Marutescu, O. Ovidiu, Design, Synthesis and Biological Evaluation of New Piperazin-4-yl-(acetylthiazolidine-2,4-dione) Norfloxacin Analogues as Antimicrobial Agents, *Molecules*. 24 (2019) 3959. <https://doi.org/10.3390/molecules24213959>.
- [6] N. Khan, S. Ahmed, I. Farooqi, Prof. I. Ali, V. Vambol, F. Changani khorasgani, M. Yousefi, S. Vambol, S. Khan, A. Khan, Occurrence, Sources and Conventional Treatment Techniques for various antibiotics present in hospital wastewaters: A critical review, *TrAC Trends Anal. Chem.* 129 (2020) 115921. <https://doi.org/10.1016/j.trac.2020.115921>.
- [7] N. Fang, Q. He, L. Sheng, Y. Xi, L. Zhang, H. Liu, H. Cheng, Toward broader applications of iron ore waste in pollution control: Adsorption of norfloxacin, *J. Hazard. Mater.* 418 (2021) 126273. <https://doi.org/10.1016/j.jhazmat.2021.126273>.

- [8] X. Yuan, J. Hu, S. Li, M. Yu, Occurrence, fate, and mass balance of selected pharmaceutical and personal care products (PPCPs) in an urbanized river, *Environ. Pollut.* 266 (2020) 115340. <https://doi.org/10.1016/j.envpol.2020.115340>.
- [9] Y. Wang, J. Lu, J. Engelstädter, S. Zhang, P. Ding, M. Likai, Z. Yuan, P. Bond, J. Guo, Non-antibiotic pharmaceuticals enhance the transmission of exogenous antibiotic resistance genes through bacterial transformation, *ISME J.* 14 (2020) 1–18. <https://doi.org/10.1038/s41396-020-0679-2>.
- [10] M. Chen, D. Wei, F. Wang, J. Yin, M. Li, Y. Du, Bioassay- and QSAR-based screening of toxic transformation products and their formation under chlorination treatment on levofloxacin, *J. Hazard. Mater.* 414 (2021) 125495. <https://doi.org/10.1016/j.jhazmat.2021.125495>.
- [11] E. Duarte, M. Oliveira, M. Spaolonzi, H. Costa, T. Silva, M. Silva, M. Vieira, Adsorption of pharmaceutical products from aqueous solutions on functionalized carbon nanotubes by conventional and green methods: A critical review, *J. Clean. Prod.* 372 (2022) 133743. <https://doi.org/10.1016/j.jclepro.2022.133743>.
- [12] S. Shur, P. T.H, T. Altahtamouni, Review on the Visible Light Photocatalysis for the Decomposition of Ciprofloxacin, Norfloxacin, Tetracyclines, and Sulfonamides Antibiotics in Wastewater, *Catalysts.* 11 (2021) 437. <https://doi.org/10.3390/catal11040437>.
- [13] C. Wang, G. Yu, H. Chen, J. Wang, Degradation of norfloxacin by hydroxylamine enhanced Fenton system: Kinetics, mechanism and degradation pathway, *Chemosphere.* 270 (2020) 129408. <https://doi.org/10.1016/j.chemosphere.2020.129408>.
- [14] S. Wohlmuth da Silva, E. Ortega, M.A. Rodrigues, A. Bernardes, V. Pérez-Herranz, The role of the anode material and water matrix in the electrochemical oxidation of norfloxacin, *Chemosphere.* 210 (2018) 615–623. <https://doi.org/10.1016/j.chemosphere.2018.07.057>.
- [15] G. Che, Q. Zhang, L. Lin, W. Chen, X. Li, Unraveling influence of metal species on norfloxacin removal by mesoporous metallic silicon adsorbent, *Environ. Sci. Pollut. Res.* 27 (2020). <https://doi.org/10.1007/s11356-020-09829-3>.
- [16] L. Molina-Calderón, C. Basualto-Flores, V. Paredes, D. Venegas-Yazigi, Advances of magnetic nanohydrometallurgy using superparamagnetic nanomaterials as rare earth ions adsorbents: A grand opportunity for sustainable rare earth recovery, *Sep. Purif. Technol.* 299 (2022) 121708. <https://doi.org/10.1016/j.seppur.2022.121708>.
- [17] N. Truc, V. Hien, B. Nguyen, N.D. Dat, B. Trung, X. Nguyen, T. Tran, T.-N.-C. Le, H. Duong, H. Bui, C.-D. Dong, X.-T. Bui, Adsorption of norfloxacin from aqueous solution on biochar derived from spent coffee ground: Master variables and response surface method optimized adsorption process, *Chemosphere.* (2022) 132577. <https://doi.org/10.1016/j.chemosphere.2021.132577>.
- [18] X. Peng, F. Hu, T. Zhang, F. Qiu, H. Dai, Amine-functionalized magnetic bamboo-based activated carbon adsorptive removal of ciprofloxacin and norfloxacin: A batch and fixed-bed column study, *Bioresour. Technol.* 249 (2017). <https://doi.org/10.1016/j.biortech.2017.10.095>.
- [19] A. Parashar, S. Sikarwar, R. Jain, Studies on Adsorption Kinetics of Norfloxacin Using Nano Alumina in Aqueous Medium, *Anal. Chem. Lett.* 10 (2020) 227–239. <https://doi.org/10.1080/22297928.2020.1775698>.
- [20] I. Rubashvili, L. Eprikashvili, T. Kordzakhia, M. Zautashvili, N. Pirtskhalava, M. Dzagania, Adsorptive Removal Study of the Frequently Used Fluoroquinolone Antibiotics -Moxifloxacin and

- Norfloxacin from Wastewaters using Natural Zeolites, *Mediterr. J. Chem.* 9 (2019) 142–154. <https://doi.org/10.13171/mjc92190921700ar>.
- [21] B. Wang, Y. Jiang, F. Li, D. Yang, Preparation of biochar by simultaneous carbonization, magnetization and activation for norfloxacin removal in water, *Bioresour. Technol.* 233 (2017). <https://doi.org/10.1016/j.biortech.2017.02.103>.
- [22] F. Okibe, C. Chinweuba Onoyima, PREPARATION AND CHARACTERIZATIONS OF HYDROXYAPATITE-SODIUM ALGINATE NANOCOMPOSITES FOR BIOMEDICAL APPLICATIONS, 2 (2022) 68–81.
- [23] T. Varadavenkatesan, V. Ramesh, S. Pai, B. Kathirvel, A. Pugazhendhi, R. Selvaraj, Synthesis, biological and environmental applications of hydroxyapatite and its composites with organic and inorganic coatings, *Prog. Org. Coat.* 151 (2021) 106056. <https://doi.org/10.1016/j.porgcoat.2020.106056>.
- [24] K. Mosaad, K. Shoueir, A. Saied, M. Dewidar, New Prospects in Nano Phased Co-substituted Hydroxyapatite Enrolled in Polymeric Nanofiber Mats for Bone Tissue Engineering Applications, *Ann. Biomed. Eng.* 49 (2021). <https://doi.org/10.1007/s10439-021-02810-2>.
- [25] S. Pai, M.S. Kini, R. Selvaraj, A. Pugazhendhi, A review on the synthesis of hydroxyapatite, its composites and adsorptive removal of pollutants from wastewater, *J. Water Process Eng.* 38 (2020) 101574. <https://doi.org/10.1016/j.jwpe.2020.101574>.
- [26] A. Nayak, B. Bhushan, Hydroxyapatite as an advanced adsorbent for removal of heavy metal ions from water: Focus on its applications and limitations, *Mater. Today Proc.* 46 (2021). <https://doi.org/10.1016/j.matpr.2021.02.149>.
- [27] K. Kandori, M. Oketani, M. Wakamura, Effects of Ti(IV) substitution on protein adsorption behaviors of calcium hydroxyapatite particles, *Colloids Surf. B Biointerfaces.* 101C (2012) 68–73. <https://doi.org/10.1016/j.colsurfb.2012.06.017>.
- [28] M. Du, J. Chen, K. Liu, H. Xing, C. Song, Recent advances in biomedical engineering of nano-hydroxyapatite including dentistry, cancer treatment and bone repair, *Compos. Part B Eng.* 215 (2021) 108790. <https://doi.org/10.1016/j.compositesb.2021.108790>.
- [29] R.H. Myers, D.C. Montgomery, C. Anderson-Cook, *Response Surface Methodology: Process and Product Optimization Using Designed Experiments*, 705 (2016).
- [30] U. Sahu, S. Mahapatra, R. Patel, Application of Box–Behnken Design in response surface methodology for adsorptive removal of arsenic from aqueous solution using CeO₂/Fe₂O₃/graphene nanocomposite, *Mater. Chem. Phys.* 207 (2017). <https://doi.org/10.1016/j.matchemphys.2017.11.042>.
- [31] A. Gugushe, A. Nqombolo, P. Nomngongo, Application of Response Surface Methodology and Desirability Function in the Optimization of Adsorptive Remediation of Arsenic from Acid Mine Drainage Using Magnetic Nanocomposite: Equilibrium Studies and Application to Real Samples, *Molecules.* 24 (2019) 1792. <https://doi.org/10.3390/molecules24091792>.
- [32] M. Boulahbal, M. Malouki, M. Canle, Z. Redouane-Salah, D. S., M. AlSalhi, M. Berkani, Removal of the industrial azo dye crystal violet using a natural clay: Characterization, kinetic modeling, and RSM optimization, *Chemosphere.* 306 (2022) 135516. <https://doi.org/10.1016/j.chemosphere.2022.135516>.

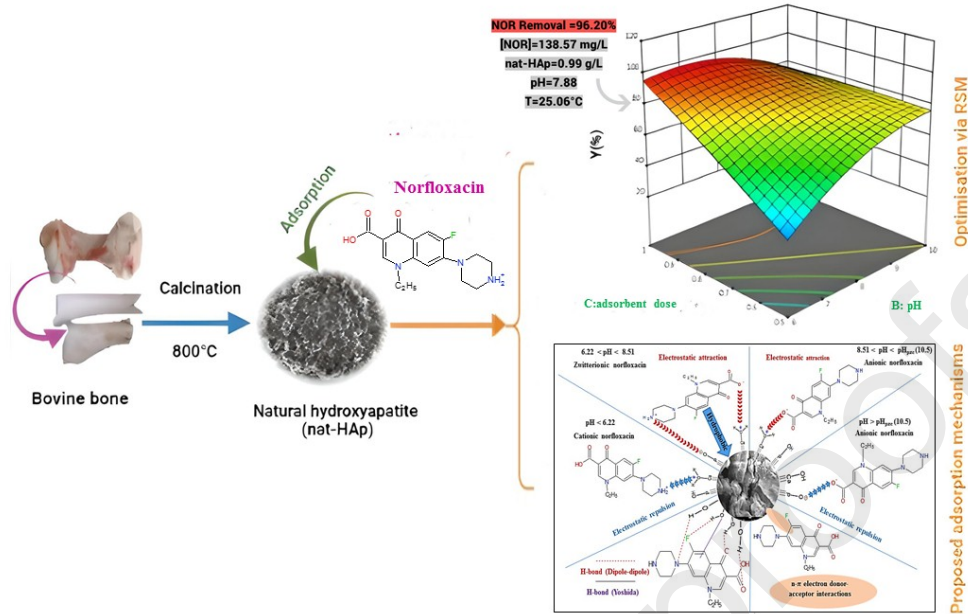
- [33] P. Hongsawat, S. Bungokule, B. Boonchouy, P. Prarat, P. Punyapalaku, Response surface methodology approach for optimization of norfloxacin by the graphene oxide under the presence of tannic acid and its adsorption mechanism, *DESALINATION WATER Treat.* 217 (2021) 272–285. <https://doi.org/10.5004/dwt.2021.26865>.
- [34] S. Cheikh, A. Imessaoudene, J.C. Bollinger, A. Hadadi, A. Manseri, A. Bouzaza, A. Assadi, A. Amrane, M. Zamouche, A. EL Jery, L. Mouni, Complete elimination of the ciprofloxacin antibiotic from water by the combination of adsorption-Photocatalysis process using natural hydroxyapatite and TiO_2 , *Catalysts* 13 (2023) 336. <https://doi.org/10.3390/catal13020336>.
- [35] M. Rana, N. Akhtar, S. Asaduzzaman, M. Hasan, Extraction and characterization of hydroxyapatite from bovine cortical bone and effect of radiatio, (2017).
- [36] N. Bano, S. Adzila, S. Jikan, H. Basri, N. Kanasan, Extraction of Biological Apatite from Cow Bone at Different Calcination Temperatures: A Comparative Study, *Key Eng. Mater.* 796 (2019) 46–52. <https://doi.org/10.4028/www.scientific.net/KEM.796.46>.
- [37] B. Soo-Ling, Z. Abdul Hamid, Hydroxyapatite derived from food industry bio-wastes: Syntheses, properties and its potential multifunctional applications, *Ceram. Int.* 46 (2020). <https://doi.org/10.1016/j.ceramint.2020.04.103>.
- [38] M. Herliansyah, C. Muzafar, A. Tontowi, Natural Bioceramics Bone Graft: A Comparative Study of Calcite Hydroxyapatite, Gypsum Hydroxyapatite, Bovine Hydroxyapatite and Cuttlefish Shell Hydroxyapatite, 2012.
- [39] Z. Movasaghi, B. Yan, C. Niu, Adsorption of ciprofloxacin from water by pretreated oat hulls: Equilibrium, kinetic, and thermodynamic studies, *Ind. Crops Prod.* 127 (2019) 237–250. <https://doi.org/10.1016/j.indcrop.2018.10.051>.
- [40] A. Imessaoudene, S. Cheikh, J.C. Bollinger, L. Belkhiri, A. Tiri, A. Bouzaza, A. El Jery, A. Assadi, A. Amrane, L. Mouni, Zeolite waste characterization and use as low cost, ecofriendly, and sustainable material for malachite green and methylene blue dyes removal: Box–Behnken Design, kinetics, and thermodynamics, *Appl. Sci.* 12(2022) 7587. <https://doi.org/10.3390/app12157587>.
- [41] L. Terskaya, I. Slesarchuk, Harrington Desirability Function for Multi-Attribute Outdoor Space Quality Assessment, *IOP Conf. Ser. Mater. Sci. Eng.* 753 (2020) 082030. <https://doi.org/10.1088/1757-899X/753/8/082030>.
- [42] G. Derringer, S. RR, Simultaneous Optimization of Several Response Variable, 12 (1980). <https://doi.org/10.1080/00224065.1980.11980968>.
- [43] B. Sadhukhan, N. Mondal, S. Chattoraj, Optimisation using central composite design (CCD) and the desirability function for sorption of methylene blue from aqueous solution onto Lemna major, *Karbala Int. J. Mod. Sci.* 2 (2016). <https://doi.org/10.1016/j.kijoms.2016.03.005>.
- [44] M. Mourabet, E.R. Abdelhadi, H. EL Boujaady, M. Bennani-Ziatni, R. El Hamri, T. Abderrahim, Removal of fluoride from aqueous solution by adsorption on Apatitic tricalcium phosphate using Box–Behnken design and desirability function, *Appl. Surf. Sci.* 258 (2012) 4402–4410. <https://doi.org/10.1016/j.apsusc.2011.12.125>.
- [45] M. Thommes, K. Kaneko, A. Neimark, J. Olivier, F. Rodriguez-Reinoso, J. Rouquerol, K. Sing, Physisorption of gases, with special reference to the evaluation of surface area and pore size

- distribution (IUPAC Technical Report), *Pure Appl. Chem.* 87 (2015). <https://doi.org/10.1515/pac-2014-1117>.
- [46] P. Sharma, H. Laddha, M. Agarwal, R. Gupta, Selective and effective adsorption of malachite green and methylene blue on a non-toxic, biodegradable, and reusable fenugreek galactomannan gum coupled MnO₂ mesoporous hydrogel, *Microporous Mesoporous Mater.* 338 (2022) 111982. <https://doi.org/10.1016/j.micromeso.2022.111982>.
- [47] Y. Yuan, F. Cai, L. Yang, Pore structure characteristics and fractal structure evaluation of medium- and high-rank coal, *Energy Explor. Exploit.* 40 (2021) 014459872110343. <https://doi.org/10.1177/01445987211034315>.
- [48] S. Chouikh, S. Cheikh, A. Imessaoudene, L. Mouni, A. Amrane, A. Benahmed, N. Bettahar, Synthesis and characterization of the carbonate hydroxalcalites (NiAl-HT, CoAl-HT, and NiCoAl-HT), and its application for removal of the anionic azo dye titan yellow from aqueous solution, *Sustainability*.15 (2023) 7948. <https://doi.org/10.3390/su15107948>
- [49] C. Piccirillo, R.A. Pinto, D. Tobaldi, R. Pullar, J.A. Labrincha, M. Pintado, P. Castro, Light induced antibacterial activity and photocatalytic properties of Ag/Ag₃PO₄ -based material of marine origin, *J. Photochem. Photobiol. Chem.* 296 (2015) 40–47. <https://doi.org/10.1016/j.jphotochem.2014.09.012>.
- [50] S. Karoui, R. Ben Arfi, K. Mougin, A. Ghorbal, A. Amrane, Synthesis of novel biocomposite powder for simultaneous removal of hazardous ciprofloxacin and methylene blue: Central composite design, kinetic and isotherm studies using Brouers-Sotolongo family models, *J. Hazard. Mater.* 387 (2019) 121675. <https://doi.org/10.1016/j.jhazmat.2019.121675>.
- [51] P. Sharma, M. Sharma, H. Laddha, R. Gupta, M. Agarwal, Non-toxic and biodegradable κ-carrageenan/ZnO hydrogel for adsorptive removal of norfloxacin: Optimization using response surface methodology, *Int. J. Biol. Macromol.* 238 (2023) 124145. <https://doi.org/10.1016/j.ijbiomac.2023.124145>.
- [52] F. Sotomayor, K. Cychosz, M. Thommes, *Characterization of Micro/Mesoporous Materials by Physisorption: Concepts and Case Studies*, (2018).
- [53] S. Joschek, B. Nies, R. Krotz, A. Göferich, Chemical and Physicochemical Characterization of Porous Hydroxapatite Ceramics Made of Natural Bone, *Biomaterials.* 21 (2000) 1645–58. [https://doi.org/10.1016/S0142-9612\(00\)00036-3](https://doi.org/10.1016/S0142-9612(00)00036-3).
- [54] W. Chen, X. Li, Z. Pan, Y. Bao, S. Ma, Efficient adsorption of Norfloxacin by Fe-MCM-41 molecular sieves: Kinetic, isotherm and thermodynamic studies, *Chem. Eng. J.* 281 (2015) 397–403. <https://doi.org/10.1016/j.cej.2015.06.121>.
- [55] S. Sahoo, C. Chakraborti, P. Behera, S. Mishra, FTIR and Raman Spectroscopic Investigations of a Norfloxacin/Carbopol934 Polymeric Suspension, *J. Young Pharm. JYP.* 4 (2012) 138–45. <https://doi.org/10.4103/0975-1483.100017>.
- [56] D. Feng, H. Yu, H. Deng, F. Li, C. Ge, Adsorption Characteristics of Norfloxacin by Biochar Prepared by Cassava Dreg: Kinetics, Isotherms, and Thermodynamic Analysis, *BioResources.* 10 (2015). <https://doi.org/10.15376/biores.10.4.6751-6768>.

- [57] F. Sher, E. Lima, I. Anastopoulos, H. Tran, A. Hosseini-Bandegharai, Is one performing the treatment data of adsorption kinetics correctly?, *J. Environ. Chem. Eng.* (2020) 104813. <https://doi.org/10.1016/j.jece.2020.104813>.
- [58] H. Tran, S.-J. You, A. Hosseini-Bandegharai, H.-P. Chao, Mistakes and inconsistencies regarding adsorption of contaminants from aqueous solutions: A critical review, *Water Res.* 120 (2017) 88–116. <https://doi.org/10.1016/j.watres.2017.04.014>.
- [59] L. Mouni, L. Belkhir, J.-C. Bollinger, A. Bouzaza, A. Tiri, F. Dahmoune, K. Madani, H. Remini, Removal of Methylene Blue from aqueous solutions by adsorption on Kaolin: Kinetic and equilibrium studies, *Appl. Clay Sci.* 153 (2018) 38–45. <https://doi.org/10.1016/j.clay.2017.11.034>.
- [60] A. Imessaoudene, S. Cheikh, A. Hadadi, N. Hamri, J.C. Bollinger, A. Amrane, H. Tahraoui, A. Manseri, L. Mouni, Adsorption performance of zeolite for the removal of congo red dye: Factorial Design Experiments, kinetic, and equilibrium studies, *Separation.* 10 (2023) 57. <https://doi.org/10.3390/separations10010057>
- [61] R. Li, Z. Wang, X. Zhao, X. Li, X. Xie, Magnetic biochar-based manganese oxide composite for enhanced fluoroquinolone antibiotic removal from water, *Environ. Sci. Pollut. Res.* 25 (2018). <https://doi.org/10.1007/s11356-018-3064-1>.
- [62] H. Tang, W. Li, J. Haishun, R. Lin, Z. Wang, J. Wu, G. He, P. Shearing, D. Brett, ZIF-8-Derived Hollow Carbon for Efficient Adsorption of Antibiotics, *Nanomaterials.* 9 (2019) 117. <https://doi.org/10.3390/nano9010117>.
- [63] X. Fang, S. Wu, Y. Wu, W. Yang, Y. Li, J. he, P. Hong, M. Nie, C. Xie, Z. Wu, Z. Kaisheng, L. Kong, J. Liu, High-efficiency adsorption of norfloxacin using octahedral UiO-66-NH₂ nanomaterials: Dynamics, thermodynamics, and mechanisms, *Appl. Surf. Sci.* 518 (2020) 146226. <https://doi.org/10.1016/j.apsusc.2020.146226>.
- [64] J. Zhou, Q. Sun, Sodium Alginate/Modified Bentonite Composite Bead Adsorptive Removal of Norfloxacin: Static and Dynamic Adsorption, *Polymers.* 14 (2022) 3984. <https://doi.org/10.3390/polym14193984>.
- [65] G.G. Haciosmanoğlu, M. Arenas, C. Mejías, J. Martín Bueno, J. Santos, I. Aparicio, E. Alonso, Adsorption of Fluoroquinolone Antibiotics from Water and Wastewater by Colemanite, *Int. J. Environ. Res. Public Health.* 20 (2023) 2646. <https://doi.org/10.3390/ijerph20032646>.
- [66] S. Varala, V. Ravisankar, M. Alali, M. Pownceby, R. Parthasarathy, S. Bhargava, Process optimization using response surface methodology for the removal of thorium from aqueous solutions using rice-husk, *Chemosphere.* 237 (2019) 124488. <https://doi.org/10.1016/j.chemosphere.2019.124488>.
- [67] M. Laabd, Y. Brahmi, B. El Ibrahim, A. Hsini, E.M. Toufik, Y. Abdellaoui, H. Abou Oualid, M. Ouardi, A. Albourine, A novel mesoporous Hydroxyapatite@Montmorillonite hybrid composite for high-performance removal of emerging Ciprofloxacin antibiotic from water: Integrated experimental and Monte Carlo computational assessment, *J. Mol. Liq.* (2021) 116705. <https://doi.org/10.1016/j.molliq.2021.116705>.
- [68] Y. Chen, T. Lan, L. Duan, F. Wang, B. Zhao, S. Zhang, W. Wei, Adsorptive Removal and Adsorption Kinetics of Fluoroquinolone by Nano-Hydroxyapatite, *PloS One.* 10 (2015) e0145025. <https://doi.org/10.1371/journal.pone.0145025>.

- [69] N. Medellin-Castillo, R. Ramos, E. Padilla, R. Ocampo, J.V. Flores-Cano, M. Berber Mendoza, Adsorption capacity of bone char for removing fluoride from water solution. Role of hydroxyapatite content, adsorption mechanism and competing anions, *J. Ind. Eng. Chem.* 20 (2014) 4014–4021. <https://doi.org/10.1016/j.jiec.2013.12.105>.
- [70] J. Wang, Z. Ming, R. Zhou, J. Li, W. Zhao, J. Zhou, Adsorption characteristics and mechanism of norfloxacin in water by γ -Fe₂O₃@BC, *Water Sci. Technol.* 82 (2020). <https://doi.org/10.2166/wst.2020.078>.
- [71] M. Moustafa, Preparation and characterization of low-cost adsorbents for the efficient removal of malachite green using response surface modeling and reusability studies, *Sci. Rep.* 13 (2023). <https://doi.org/10.1038/s41598-023-31391-4>.
- [72] E. Lima, A. Hosseini-Bandegharaei, J. Moreno-Piraján, I. Anastopoulos, A critical review of the estimation of the thermodynamic parameters on adsorption equilibria. Wrong use of equilibrium constant in the Van't Hoof equation for calculation of thermodynamic parameters of adsorption, *J. Mol. Liq.* 273 (2018). <https://doi.org/10.1016/j.molliq.2018.10.048>.
- [73] H. Tran, Improper estimation of thermodynamic parameters in adsorption studies with distribution coefficient KD (q_e/C_e) or Freundlich constant (KF): Conclusions from the derivation of dimensionless thermodynamic equilibrium constant and suggestions, *Adsorpt. Sci. Technol.* (2022). <https://doi.org/10.1155/2022/5553212>.
- [74] M. Sui, Y. Zhou, L. Sheng, B. Duan, Adsorption of norfloxacin in aqueous solution by Mg–Al layered double hydroxides with variable metal composition and interlayer anions, *Chem. Eng. J.* 210 (2012) 451–460. <https://doi.org/10.1016/j.cej.2012.09.026>.
- [75] H. Li, D. Zhang, X. Han, B. Xing, Adsorption of antibiotic ciprofloxacin on carbon nanotubes: PH dependence and thermodynamics, *Chemosphere.* 95 (2013). <https://doi.org/10.1016/j.chemosphere.2013.08.053>.
- [76] Md.A. Islam, Z. Nikoloutsou, V. Sakkas, M. Papatheodorou, T. Albanis, Statistical optimisation by combination of response surface methodology and desirability function for removal of azo dye from aqueous solution, *Intern J. Env. Anal. Chem.* 90 (2010) 497–509. <https://doi.org/10.1080/03067310903094503>.
- [77] H. EL Boujaady, M. Mourabet, E.R. Abdelhadi, M. Bennani-Ziatni, R. Hamri, T. Abderrahim, Interaction of adsorption of reactive yellow 4 from aqueous solutions onto synthesized calcium phosphate, *J. Saudi Chem. Soc.* 94 (2013). <https://doi.org/10.1016/j.jscs.2013.10.009>.
- [78] Md.T. Uddin, M. Rahman, M. Rukanuzzaman, Md.A. Islam, A potential low cost adsorbent for the removal of cationic dyes from aqueous solutions, *Appl. Water Sci.* (2017) 1–12. <https://doi.org/10.1007/s13201-017-0542-4>.
- [79] T. Alsawy, E. Rashad, M. El-Qelish, R. Mohammed, A comprehensive review on the chemical regeneration of biochar adsorbent for sustainable wastewater treatment, *Npj Clean Water.* 5 (2022). <https://doi.org/10.1038/s41545-022-00172-3>.
- [80] T. Robinson, G. McMullan, R. Marchant, P. Nigam, Remediation of dyes in textile effluent: A critical review on current treatment technologies with a proposed alternative, *Bioresour. Technol.* 77 (2001) 247–55. [https://doi.org/10.1016/S0960-8524\(00\)00080-8](https://doi.org/10.1016/S0960-8524(00)00080-8).

Journal Pre-proofs



Research Highlights

- nat-HAp produced by thermal calcination of bovine bone was used to remove NOR from aqueous phase.
- Optimization of process parameters using Box-Behnken design in response surface methodology.
- Adsorption of NOR onto nat-HAp takes place as monolayer adsorption.
- Adsorption of NOR onto nat-HAp was controlled by physisorption.
- Electrostatic, hydrophobic, H-bond and $n-\pi$ electron donor-acceptor interactions were the main mechanisms.
- nat-HAp was still stable after four cycling runs.

Declaration of interests

The authors declare that they have no known competing financial interests or personal relationships that could have appeared to influence the work reported in this paper.

The authors declare the following financial interests/personal relationships which may be considered as potential competing interests:

Journal Pre-proofs